LBNL-39159
UC-404
Preprint

ERNEST ORLANDO LAWRENCE BERKELEY NATIONAL LABORATORY

The β-3C to α-4H Phase Transformation and Microstructural Development in Silicon Carbide Hot Pressed with Al, B, and C Additives

W.J. MoberlyChan, J.J. Cao, and L.C. De Jonghe
Materials Sciences Division

July 1996
Submitted to *Journal of the American Ceramic Society*

REFERENCE COPY
Does Not
Circulate
Bldg. 50 Library.
LBNL-39159
Copy 1

DISCLAIMER

This document was prepared as an account of work sponsored by the United States Government. While this document is believed to contain correct information, neither the United States Government nor any agency thereof, nor the Regents of the University of California, nor any of their employees, makes any warranty, express or implied, or assumes any legal responsibility for the accuracy, completeness, or usefulness of any information, apparatus, product, or process disclosed, or represents that its use would not infringe privately owned rights. Reference herein to any specific commercial product, process, or service by its trade name, trademark, manufacturer, or otherwise, does not necessarily constitute or imply its endorsement, recommendation, or favoring by the United States Government or any agency thereof, or the Regents of the University of California. The views and opinions of authors expressed herein do not necessarily state or reflect those of the United States Government or any agency thereof or the Regents of the University of California.

LBNL-39159
UC-404

THE β–3C to α–4H PHASE TRANSFORMATION AND MICROSTRUCTURAL DEVELOPMENT IN SILICON CARBIDE HOT PRESSED WITH Al, B, & C ADDITIVES

W. J. MoberlyChan,
J. J. Cao, and L. C. De Jonghe

Department of Materials Science and Mineral Engineering,
University of California

and

MATERIALS SCIENCES DIVISION
Lawrence Berkeley National Laboratory
University of California
Berkeley, CA 94720

JULY, 1996

This work was supported by the Director, Office of Energy Research, Office of Basic Energy Sciences, Materials Sciences Division, of the U. S. Department of Energy under Contract No. DE-AC03-76SF00098.

The β–3C to α–4H Phase Transformation and Microstructural Development in Silicon Carbide Hot Pressed with Al, B, & C Additives

W. J. MoberlyChan[1], J. J. Cao[2], and L. C. De Jonghe[2]
[1]Center for Advanced Materials, Lawrence Berkeley Laboratory, Berkeley, CA 94720
[2]Department of Materials Science and Mineral Engineering,
University of California at Berkeley, Berkeley, CA 94720

ABSTRACT

The beta-3C to alpha-4H phase transformation in SiC, hot pressed with <5% total Al, B, and C additions, occurs via a growth of the hexagonal phase out of the initial submicron, cubic seed grain. The propensity of parallel stacking faults in the initial beta grain results in anisotropic growth of the beta grain, which develops a switch-over in stacking to the alpha-4H structure as it grows at temperatures above 1700°C. The anisotropy of the 4H structure enhances elongated growth to form plate-like, dual-phase grains, with an atomically flat top terminating the alpha phase and an irregular, faceted bottom terminating the beta phase. Subsequent growth above 1850°C develops an interlocking, plate-like microstructure, with high toughness ($K_c > 9$ MPa $m^{1/2}$) and high strength (> 700 MPa); yet the initial beta seed portion of the grain is retained. Although motion of grain boundaries and grain shapes are strongly influenced by interface attachment kinetics regulated by a ~1 nm thick liquid phase, the macroscopic driving force is akin to Ostwald ripening. Partial dislocation motion is not operative in this growth-induced transformation. The complex crystal structures, microstructures, and secondary phases require an interactive XRD, SEM, and HR-TEM analysis; and reevaluations of other individual datum reported for polycrystalline SiC are consistent with this growth-induced transformation mechanism.

INTRODUCTION

The beta-to-alpha phase transformation in SiC was originally classified as a recrystallization mechanism dominated by vapor transport between crystallites [1, 2, 3]. Subsequent development in single crystal growth led to the identification of a transformation mechanism using stacking faults to propagate the cubic to hexagonal transformation [4, 5, 6], with recent work by Pirouz and Yang presenting high resolution TEM evidence and models of dislocation-induced transformation in single crystals [7]. The numerous recent studies of transformations in polycrystalline SiC typically have referenced a series of papers by Heuer *et al.* [8-11] as providing the most complete analysis of the transformation and developing microstructure in SiC. Their transformation was interpreted as invoking the same mechanisms that have been theorized and observed in single (or large) crystal SiC and other zincblende structures [3, 6, 7, 12-16], in particular a solid state transformation involving the motion of partial dislocations and stacking faults to invoke a change in structure. In the seminal work by Heuer *et al.* [8-11], polycrystalline SiC transformed upon heating from the 3C-beta phase (with the zincblende $A\alpha B\beta C\gamma A\alpha B\beta C\gamma$.... stacking) to the 6H-alpha phase (with the $A\alpha B\beta C\gamma A\alpha C\gamma B\beta A\alpha B\beta C\gamma A\alpha C\gamma B\beta$.... stacking), which has typically been accepted as the theoretical equilibrium high temperature phase [14, 17, 18]. Transformations to other polytypes (such as 15R, 4H, or 2H) have also been observed [12-16, 19-32], and even the reverse transformation from alpha to beta at high temperature, under conditions of applied stress or pressure, has been discussed [6, 15, 20, 33, 34]. (The C, H, and R refer to cubic, hexagonal, and rhombohedral crystal structures, and the preceding number is the Ramsdell notation [35], which corresponds to the number of Si-C tetrahedral layers in a unit cell of each structure. Detailed descriptions of crystal structures and stacking notations in SiC are provided in references [7, 14, 15].) The many differences in transformation products can be attributed to different impurities, often intentionally added to aid sintering of polycrystalline SiC from powders; and some differences in the final structure may also relate to the processing conditions [8-16, 19-32, 36-45].

Due to a renewed interest in improving the mechanical properties of SiC, the recent literature has numerous observations of microstructural changes in SiC that may be associated with the beta-to-alpha transformation [45-56]. However, the majority of these recent articles do not present a TEM analysis of the microstructure; most do not present XRD data, which can be fraught with misinterpretation of the polytype(s) present [15, 57-59]; and the transformation study of Heuer *et al.* [8-11] is typically cited as representative of what transformation may have occurred. It is recognized that even the preparation of samples for optical microscopy and/or SEM analysis involves difficult etching routines [60], resulting in micrographs that are not immune of misinterpretation. The majority of the afore-cited articles involving polycrystalline SiC observe the development of a plate-like microstructure and attribute this morphology to a transformation from beta cubic powders to the alpha hexagonal crystal structure. However, two articles depict elongated

microstructures and refer to XRD data that declare these materials retain the beta cubic crystal structure [61, 62]. Similarly, both plate-like and equiaxed microstructures have been reported to form when processing starts with only alpha powders [56, 63-65]. Some discrepancies in microstructural interpretation may be true differences due to additives and processing variables. The present research effort has determined that the characterization of SiC is subject to controversial interpretation, and combined analyses using many techniques are necessary to understand the microstructure and correlate it to the phase transformation and the mechanical properties [6, 44, 66-74].

The cubic-to-hexagonal transformation in polycrystalline SiC has been utilized in recent processing developments to improve the fracture toughness through the evolution of an *in situ* toughened microstructure [45-56, 61, 66]. A rising fracture resistance (R curve) [75] and a K_C in excess of 9 MPa $m^{1/2}$ (over three times that of commercially available Hexoloy SA) represent an advancement of SiC to a practical structural material. These toughened SiC ceramics have a dense, plate-like microstructure and invoke a tortuous fracture path around the elongated grains. The majority of these toughened microstructures incorporate between 5 and 20% secondary phases resulting from sintering aids [45-56, 61], and the crack path through this second phase may correlate with poor creep resistance similar to the effect large volume fractions of secondary phases have on *in situ* toughened Si_3N_4 materials [76, 77, 78]. However, mechanical testing of a SiC with <4% secondary phases promise neither high temperature properties [79] nor strength [66] have to be sacrificed to achieve this high toughness [75]. The strength actually increases as grains grow due to an increase in the interlocking of these plate-like grains [66].

This paper focuses on the transformation mechanism for a polycrystalline silicon carbide processed with Al, B, and C (hereto named ABC-SiC). For this ABC-SiC the observed transformation is from beta-3C to the alpha-4H polytype, and therefore at least the transformation product differs from that described by the Heuer papers. Since many of the studies on "*in situ* toughened" SiC report XRD analyses that indicate the transformation product is an α–4H structure [45-50], the to-be-presented transformation mechanism may be more appropriate than those described by Heuer *et al.* [8-11] and in single crystals [7]. Because of the different starting powders, additives and processing variables utilized by other research efforts, the following transformation mechanism can not be declared to be the fully general mechanism. However, it will be shown that the microstructures presented in all literature of other fine-grain SiC materials could incorporate the same cubic-to-hexagonal transformation mechanism observed in this ABC-SiC [72].

The transformation from β–3C (ABCABC....) to α–4H (ABACABAC....) has been previously reported for SiC materials that include either Al and/or alumina as an additive, [23-26, 31, 43, 45-50] and usually at a temperature lower than that of the $\beta-\alpha$ transformation for "pure" β–SiC powders [6, 16, 21] or with other additives [8-11, 13, 25, 26]. However, it is unclear whether the Al has a chemical effect [52, 80] that causes the α–4H structure to form or if the invocation of the transformation at the lower temperature

causes the 4H structure to be stable. Single crystals of α–4H have been reported to grow from melts without Al at temperatures below 2000°C [6, 81-83]; and theoretical calculations have predicted the α–4H structure is the equilibrium phase (of pure SiC) from room temperature to >1950°C [17, 18, 84, 85]. The experimental growth of the α–4H structure has also been attributed to additives other than Al [86, 87]. Conversely, the growth rates of 6H single crystals have been enhanced at temperatures below 1900°C by the addition of Al, even for amounts larger than 10% [88]. The α–4H structure is not believed to be the equilibrium structure in the present ABC-SiC for all possible processing temperatures, however it is the primary hexagonal phase observed in this study. Traces of α–6H and α–15R are detected for the higher processing temperature (1950°C) and longer processing times. These phases may be an indication of the onset of a subsequent transformation(s), from α–4H to a larger polytype [3]. Sequential transformations, based on XRD analyses, have been previously plotted as a function of processing temperature [24, 26, 83]; and mixtures of α–4H and α–6H have also been detected by electron diffraction in other SiC materials processed at 1950°C for 5 hours [51, 52]. The microstructural changes, associated with the transformation(s) between alpha polytypes are minimal, as compared to those for the beta-to-alpha transformation; and the change in mechanical properties is minimal if not detrimental [89]. Thus the nature of subsequent transformation(s), which for particular processing conditions may actually begin before the β–3C to α–4H transformation is complete, are not described in detail in this report.

Three aspects of this observed β–3C to α–4H transformation are initially circumscribed, as the processing conditions here incurred could often be intentionally altered for other SiC ceramics. These are the issues of initial grain size, seed crystals for the transformation, and the interaction of densification and transformation. The transformation observed in ABC-SiC cannot apply to (non-expanding) single crystals, nor to very large-grain beta SiC under conditions where the driving forces for grain growth (or Ostwald ripening) are negligible. Secondly, many research efforts discuss the need of alpha seeds in order to start the transformation at lower temperatures [6, 47, 48]; ranging from using >10% seed [54], to needing <2% seed in order to ensure densification [55], to having transformation occur with no alpha seed [56], with all of these three materials using alumina and yttria as the primary sintering additives. It is reasonable that the preferential "growth" of alpha seeds within a beta SiC matrix will provide a transformation that is strongly influenced by the seeds themselves. For example, α–6H seed grains may be expected to encourage the transformation product to be α–6H [63], similar to single crystal seeds [88]. On the other hand, the seed could lead to a "cored" growth process, where the grain growing around the seed has a different crystal structure and/or chemistry [8, 11, 60, 90-92]. The ABC-SiC studied in this report did not have any intentional alpha seeds, nor was any alpha phase observed in the starting powders using XRD and electron diffraction.

Densification, which is a first requirement of high toughness in a ceramic, is usually enhanced by liquid-phase sintering [93]. During processing of ABC-SiC the

microstructure develops via the transformation from submicron beta powders to a dense plate-like alpha microstructure with a grain size upwards of 10 microns in diameter. The phase transformation could be concurrent with the densification, with both being enhanced at lower temperatures by liquid-phase sintering aids. If the transformation occurs too readily before densification, the impinging elongated plates can actually prevent densification [6, 43], with this being the logic behind limiting the volume fraction of alpha seeds [55]. For the present ABC-SiC, hot pressing enables the beta SiC to be densified (>99%) at temperatures below 1700°C [44, 66], prior to the beta-to-alpha transformation. Thus the transformation can be treated as isolated from the densification process, and the transformation is occurring within a completely dense material. Based on reported discussions for processing of other SiC ceramics, such a condition is not necessarily always true [6]. Even for this ABC-SiC, however, the transformation must be dealt with as a competing process with continued grain growth in the beta matrix itself. A discussion of this "competition" was not included in the transformation mechanism presented in the Heuer papers [8-11]. And no reports exist of the phase transformation occurring with a resulting decrease in "grain" size, which is theoretically anticipated for the classic recrystallization model with nucleation on defects. (One study [32] does present evidence of localized grain refinement when AlN is used as a solid solution additive to form multiple α–2H variants within beta grains.) As will be presented, the β–3C to α–4H transformation in ABC-SiC occurs via the growth of the alpha phase from a beta "seed" grain, without consuming the beta seed; and grain growth (akin to Ostwald ripening), modified by anisotropic grain boundary energies, is the dominant kinetic process throughout the transformation.

EXPERIMENTAL PROCEDURES

In this study materials were hot pressed at temperatures ranging from 1650°C to 1950°C and for a duration of 15 minutes to 4 hours. The starting beta-SiC powders (BSC-21, Ferro, Inc., Cleveland, OH) were nominally 0.2 microns in diameter; however, the particle distribution was skewed with many powders smaller by a factor of ten and none larger than two microns. The sintering additives used in this study were 3 weight % Al, ~0.6 % B, and ~2 % C, the latter having been introduced as a larger concentration of a wax binder and partially lost during burn-out prior to densification. As noted in other works [67, 68, 74, 94], the Al sintering additive is typically introduced with a particle size >2 microns and consequently affects the size of residual secondary phase regions in the final hot pressed compact. The size of the Al additive, the volume fraction of additive(s), the processing temperature, and the soaking time are all interactive variables which control not only densification but also the transformation [69]. The concentration of additive(s) has a primary purpose to produce a dense, structurally useful ceramic, with the effect on transformation temperature being a secondary concern.

The hot pressed SiC materials were characterized by X-Ray Diffraction (XRD), Electron Diffraction, Scanning Electron Microscopy (SEM), Transmission Electron Microscopy (TEM), High Resolution TEM, and peripheral spectroscopic techniques (EDS, PEELS, Auger, etc.) to evaluate the phase transformation as a function of processing conditions. Additional characterization of the microstructure has been previously presented and correlated to the measured mechanical properties [66]. The XRD scans were acquired from polished surfaces of the sintered compacts. The present data compares well with powder patterns utilized by Ruska *et al.* [95] to determine relative volume fractions of polytypes in SiC, thereby indicating these polished surfaces provide a random distribution of grain orientations. On the other hand, preparation of powder XRD samples by insufficient grinding of plate-like, intergranularly-fracturing microstructures results in a propensity of plates parallel to the surface of the XRD pressed pellet. This in turn artificially inflates the peak representing the basal planes, which may be inappropriately measured as a high volume fraction of cubic beta phase. SEM imaging was performed on polished sections, surfaces heavily etched by molten salt [60], and on fracture surfaces. Because of the low volume fraction of secondary phase, these ABC-SiC materials required etching several hours in a molten salt bath (90% KOH and 10% KNO_3, [60]) at ~500°C in order to reveal the microstructure. Surfaces imaged using >10 KeV incident electron beam voltage required application of thin Au conductive coatings. SEM images acquired with <8 KeV and no conductive coating provided additional contrast to distinguish secondary phases. TEM analyses were performed on samples thinned from these hot pressed compacts by grinding, dimpling to <10 micron thickness, and final Ar ion milling to electron transparency. More details on the individual TEM experiments are presented with their corresponding results. (XRD analyses were

acquired with a Siemens D500. SEM imaging was performed on a Topcon ISI DS130 microscope. TEM experiments were conducted using the Philips EM400, the Topcon ISI-002B, the JEOL 200CX, and the JEOL ARM-1000 microscopes, with Energy Dispersive X-Ray and Parallel Electron Energy Loss Spectrometers utilized for chemical analyses.)

EXPERIMENTAL RESULTS & ANALYSIS

The XRD scans in Figure 1a through 1e were acquired of the initial beta SiC powders and materials hot pressed for 1 hour with 3% Al sintering additive at 1700°C, 1780°C, 1900°C, and 1950°C, respectively. These patterns were indexed [66], using the method developed by Ruska *et al.* [95], and determined to contain ~0% α–4H, 20% α–4H, 75% α–4H, and 100% α–4H for the four respective processing temperatures. No other polytypes of alpha SiC were observed by XRD; although high resolution TEM observed occasional nanometric-scale regions in some grains that exhibited 6H and 15R stacking in the ceramics processed at 1950°C. As shall be described in the TEM results, many of the grains were a combination of beta and alpha phase, but the XRD analysis does not discern this. Figure 1f plots the volume fraction transformed to α–4H as a function of processing temperature, however, transformation is a function of time and additive(s), too. As an example, 3% Al in conjunction with hot pressing 4 hours at 1900°C provided complete transformation to the alpha structure, whereas 1% Al produced negligible transformation in 1 hr at the same temperature. The interpretations possible for XRD analyses of SiC are complex due to the propensity of stacking faults and mixed polytypic phases [15, 57, 58, 59]. Thus the analysis of this XRD data is delayed until the discussion section following the description of microstructure by TEM.

Figures 2a and 2b are SEM images of the etched surfaces of two ABC-SiC materials hot pressed for 1 hour at 1700°C and 1900°C, which respectively present the microstructures at the beginning and the end of the transformation. Such etched surfaces can readily depict the grain shapes; however, these heavily etched surfaces do not present a true distribution of grain sizes. Smaller grains are more readily removed, leaving the etched surface with an artificially high density of the large grains. SiC is quite resistant to chemical attack, and generally the initial removal of secondary phases makes metallographic analysis more representative of the secondary phase microstructure rather than the SiC. Backscatter electron (channeling) contrast from polished, unetched surfaces differentiates the crystallographic orientations of the SiC grains, as well as the distribution and chemistry of secondary phases [96]. However, TEM sections present a more appropriate distribution of grain sizes, especially for submicron grains. Still the etched surfaces readily depict the plate-like shapes of the grains, especially the planar grain boundaries. The SiC in Figure 2a, which is determined by XRD and electron diffraction to consist of all cubic phase, exhibits small, "plate-like" grains. In conjunction with TEM results, these grains have a minor elongation (aspect ratio <2), but have very smooth facets on one of the (111) low-energy planes. The smaller $\{\bar{1}11\}$ facets at the ends, which are interrupted by intersecting internal faults, are not individually resolved by this SEM analysis. The presence of the large smooth (111) facet gives an overall impression of a plate-like shape. Processed at 1900°C (Figure 2b), the microstructure has grown into large, interlocked, plate-like grains, which are established by XRD and electron diffraction as containing a majority of the hexagonal phase. Additional metallographic analyses are detailed elsewhere [66, 96, 97].

Figures 3a, 4a, and 5a depict low magnification bright field TEM images of three SiC samples (with 3% Al as an additive) hot pressed at 1700°C, 1780°C and 1900°C, respectively. The first microstructure is before the transformation, the second represents the beginning of the transformation, and the microstructure at 1900°C represents the latter part of the transformation. The microstructure at 1700°C exhibits complete densification of SiC via liquid-phase-sintering, but at a sufficiently low temperature that prevents any measurable transformation of the cubic structure to a hexagonal structure. Two basic grain shapes exist at 1700°C. The larger grains have grown to ~1 micron in length, with an aspect ratio typically <2 and elongated parallel to the stacking faults and microtwins within the beta grain. These grains have flat (111) planes terminating one surface. However, much of the microstructure is comprised of fine (submicron) beta grains, with many grains similar in size to the original beta powders. Although some of these finer grains exhibit a few stacking faults and microtwins on multiple {111} types of planes, the majority exhibit only one parallel set of (111) faults. On average, substantial grain growth is established as having occurred during this initial sintering process, corresponding to a reduction in width of the (111) peak in the XRD data (Figure 1a vs. 1b). Yet, TEM imaging in Figure 3a determines that removal of all smaller grains (by processes akin to Ostwald ripening) is far from complete for the nominal 1 hour processing at 1700°C.

Figure 3b is a $[\bar{1}10]$ Selected Area Diffraction (SAD) pattern acquired of a larger SiC grain that can be presumed to have undergone some growth during the sintering process at 1700°C. It is typical for these beta SiC grains to exhibit numerous parallel (111) twins and stacking faults, as indicated by the twin reflections and streaking, respectively. Depending on the size of the analyzed region within one grain, the SAD patterns sometimes exhibit discrete reflections indicative of higher order hexagonal polytypes; however, high resolution imaging indicates a mixture of stacking faults and beta microtwins is a more appropriate assessment. Selected area diffraction has a practical resolution of 100 to 200 nm, and microdiffraction of smaller regions using a converged beam can be uncertain due to the propensity of stacking faults and the large periodicity of the alpha polytypes. Similar faults and corresponding SAD patterns have been observed for the starting beta SiC powders [67]. Although the beta SiC structure allows for a multiplicity of four equivalent {111} planes, four sets of different growth twins are not typically observed within any one grain. These commonly observed [8, 12] parallel faults, which typically extend the entire length of the grain, disrupt the overall cubic symmetry of a beta grain and cause anisotropic growth (see section *ii* in discussion).

The microstructure of the 1780°C material exhibits three basic grain morphologies. Much of the microstructure still is comprised of fine (submicron) beta grains. The larger beta grains have grown to 1-2 microns, again with an aspect ratio typically <2. The third type of grain is larger and with a higher aspect ratio, as represented by the grain oriented for strong diffraction contrast in Figure 4a. Although a typical TEM section implies these larger grains are few and isolated, SEM micrographs [66, 97] of etched surfaces indicate

these long plate-like grains often impinge upon one another. Figures 4b through 4d are SAD patterns acquired from the three sequential regions of this diffracting grain. Whereas the bottom part of the grain exhibits the $[\bar{1}10]$ zone axis of the beta phase (Figure 4b), the upper third of the grain exhibits the $[\bar{2}110]$ zone axis of the 4H-alpha phase (Figure 4d). Diffraction from the middle portion of the grain (Figure 4c) exhibits twin reflections indicative of $(111)_{\beta-3C}$ twinning and streaking due to a high density of $(111)_{\beta-3C}$ and $(0001)_{\alpha-4H}$ stacking faults. Within the streaking in the diffraction pattern of Figure 4c (and similar regions), weak superlattice reflections are visible, which could be identified as various large-stacking hexagonal polytypes [98, 13]. Although these superlattice reflections imply a mixture of large-stacking polytypes, high resolution imaging determines these larger polytypes do not exhibit repeated stacking arrangement for more than 1 or 2 modulations (i.e. 1 or 2 unit cell thicknesses). Thus a graded layer of beta twins, stacking faults and α–4H may be a more reasonable assessment of the stacking arrangements in the middle of the grain. Crystals comprised of mixed polytypes, such as this intermediate region with a "conversion" from the cubic to the hexagonal stacking, have been referred to as a "one-dimensionally disordered" in both HR-TEM [58, 99] and XRD experiments [23, 100].

All larger elongated grains in this 1780°C material (Figure 4a) exhibit this "dual phase" structure, when analyzed by electron diffraction. Whereas XRD (Figure 1c) indicates only a small volume fraction of α–4H exists, metallographic images [66, 72, 97] of this material indicate a substantial fraction of elongated, "plate-like" grains are present. These two conflicting datum are resolved by the TEM determining the presence of these dual-phase grains. A typical TEM image (Figure 4a) has only a couple plate-like grains sectioned such that their elongated nature is apparent, and TEM data appears to coincide with the XRD assessment of a small volume fraction of alpha phase. However, with grains determined to be dual phase, and with the high density of stacking faults reducing the apparent XRD volume fraction of α–4H, a much larger fraction of plate-like grains must exist. Thus the SEM micrographs [97] overestimate the microstructure as >50% plate-like grains, while the ~20% transformed to the α–4H is underestimated by XRD (Figure 1f). (Sections *iii* and *iv* discuss how the α–4H portion of the grain develops before the significant elongation of the grain.)

The microstructure of the 1900°C material (Figure 5a) is dominated by the larger grains, upwards of 10 microns in length, with a high aspect ratio (upwards of 10). Since the grains are "plate-like" in shape, any general sectioning to make a TEM sample of this microstructure exhibits the majority of the plate-like grains as being elongated. The bright field TEM image of Figure 5a exhibits strong diffraction contrast for a typical grain in cross section, with the grain in this case being oriented along the $[\bar{2}110]_{4H}$ zone axis. Electron diffraction, as well as high resolution imaging, again determines that such grains are partially twinned beta and partially 4H-alpha, at the bottom and top, respectively. The stacking fault density varies throughout the thickness of the grain, with a decrease in stacking faults near the top of the alpha phase [72]. In general, all grains except those sectioned normal to the plate will have their thicknesses exaggerated.

Conversely, a plate-like grain will not typically be sectioned through its middle, thereby underestimating the actual diameter of the plate-like grains. An assessment of what constitutes a true aspect ratio is difficult. An initial approach may be to measure the thicknesses only of the thinnest plates and the lengths of only the longest plates in an SEM micrograph [63]; however, it is believed a more-averaged measurement correlates with the mechanical properties [66, 69], because of the interlocking nature of this plate-like microstructure. TEM can provide a better assessment of the true thickness of a plate than can an SEM micrograph (without quantified backscattering channeling contrast [96]), because the grain can be oriented in the TEM to a zone axis parallel to the (0001) face.

This microstructure comprised of plate-like grains exhibits two subtleties regarding the shape of the grains. The first deals with the consideration that a dense material made up of plate-like grains causes the plates to develop irregular shapes as they intersect each other. The second geometrical aspect is readily apparent in both Figures 4a and 5a. The "tops" of these plate-like grains are quite flat, whereas the bottoms are quite rough. The top has the α–4H phase and the planar surface represents the only $\{0001\}$ low-energy plane in the hexagonal structure. The bottom has the β–3C phase, and the exhibited faceting occurs at angles between 35° and 70°. This indicates the facets are made up of cubic $\{\bar{1}11\}$-type, low-energy planes, with the bottom-most portions of the grain truncated by the lowest energy, step-free (111) facet. These phenomena of rough bottom surfaces and irregular shapes, as well as how they relate to both the transformation and properties, will be further discussed in sections *v*, *vi*, and *vii*.

The inset high resolution TEM image (Figure 5b) exhibits the 4H stacking as imaged along a $\langle\bar{2}110\rangle$ zone axis orientation. In addition to exhibiting the planar nature of the top 4H-alpha surfaces of these elongated grains, high resolution imaging depicts the presence of a thin (nominally 1 nm thick) amorphous layer along the grain boundaries. Amorphous grain boundaries also have been observed on other grain boundaries in these ABC-SiC materials and have been discussed in more detail elsewhere [66, 73, 105]. Triple points smaller than a few nanometers exhibit an amorphous nature, as indicated in the high resolution image of Figure 5b. On the other hand, larger triple points exhibit a primarily crystalline nature, as is evident by the diffraction contrast denoted by the arrow in Figure 5a. The triple points, amorphous layers, and planar grain boundaries all play an integral role with the plate-like grain shapes to promote high toughness in these SiC materials [66, 69, 73].

HR-TEM can clearly present the atomic stacking arrangements to define each polytype and locate each individual stacking faults; however, the difficulties in acquiring experimental high resolution images of SiC polytypes are further complicated by their difficult interpretation [101, 102]. HR-TEM imaging provides a more discriminating analysis than BF-TEM imaging or selected area electron diffraction to establish which polytypes are present throughout all layers of these plate-like grains [72]. Some past studies of SiC microstructures have presented high resolution images that do not contain cross fringes [52, 98, 99, 100, 103]; however, resolving a particular stacking polytype amongst the high density of stacking faults in such images is difficult. Early HR-TEM

assessments [98] of stacking variants of 5, 7, etc. basal planes are now recognized as not representing repeatable polytypes [85]. Yet lattice imaging, combined with electron diffraction, has been recognized to be the most certain means to characterize the internal structure of SiC crystals [58, 100, 101, 104]. The $\langle\bar{2}110\rangle$ orientation (Figure 5b) in a high resolution image is the only one which can typically resolve which polytype is present because it images the $(0\bar{1}10)$ planes. The other low index zone, which encompasses the (0001) plane, is the $\langle 0\bar{1}10\rangle$, and the 0.15 nm spacing of the $(\bar{2}110)$ cross fringes are not easily resolved by most high resolution microscopes. Thus the $\langle 0\bar{1}10\rangle$ orientation does not provide useful high resolution imaging for establishing what polytype(s) is(are) present. Similarly, the hexagonal $\langle\bar{2}110\rangle$ zone axis selected area diffraction pattern is readily discerned from the corresponding <011> cubic zone axis (see Figures 4b and 4d), whereas the $\langle 0\bar{1}10\rangle$ hexagonal and corresponding <112> cubic zone-axis SAD patterns are basically indistinguishable.

HR-TEM images, which resolve cross lattice fringes, enable the discrimination of single-layer faults, microtwins, and different polytypes a few planes thick. Although diffractograms (optical [98] and/or computer-generated FFT's [69, 105]) can measure stacking modulations of many polytypes, the direct imaging of the stacking sequences indicate a more appropriate assessment is a random arrangement of stacking faults and microtwins in the lower beta portion of the grains, and mixed alpha-4H and beta in the "conversion" region in the middle of the grains. For example, a 1-unit-cell-thick "5H" variant is more appropriately measured as parts of 4H and 3C regions; yet the continuity of these planar faults across a 10-micron grain provides sufficient material to generate reflections in a diffractogram (or SAD pattern). In addition to differentiating phases, a HR-TEM image with cross fringes can assess the relative distribution of stacking faults throughout the grain thickness. Stacking faults are less common in the α–4H structure than in the β–3C portions of the grain. Additionally, the stacking fault density is most reduced near the topmost layers of the α–4H region. Contrasting the fault density in grains similar to those imaged in Figures 4a and 5a determine the portions of alpha regions grown at higher temperatures also have less stacking faults [72]. Furthermore, the conversion region, which contains mixed stacking of α–4H and β–3C in the middle of the grain, exhibits a higher density of faults than the beta region that grew below it. Although a qualitative assessment is made of the variation in stacking faults density through the thickness of a dual-phase grain, attempts to quantify the limited volumes sampled by HR-TEM have not yet been fruitful.

When hot pressed at 1950°C for 1 hour (Figure 6a) or 1900°C for 4 hours (Figure 7a), the cubic-to-hexagonal transformation is nearly complete. XRD analysis (Figure 1e) indicates the material is 100% α–4H, and microstructural imaging determines all grains have a plate-like shape. However, TEM analysis of the "bottoms" of grains establishes the presence of residual beta regions (Figure 7a). A typical section (Figure 6a) determines the grains are substantially larger as compared to 1900°C for 1 hour (Figure 5a), but also indicates a lower aspect ratio is a consequence of higher processing temperatures [66, 69]. (This reduction in aspect ratio and its detrimental affects on

mechanical properties, as well as the voids at small triple points in Figures 6a and 6b, are discussed in an article on "oversintering" [89].) Only for an exactly cross-sectioned grain can the beta "bottoms" be readily viewed. The diffracting grain in Figure 7a, which has been oriented along the [$\bar{2}110$] zone axis, exhibits the typical planar top surface and the irregular bottom surface. Figure 7b is an SAD pattern determining the 4H structure exists within the majority of the grain. Although stacking faults are evidenced by the minor streaking in the diffraction pattern, they are not readily visible in a bright field image when the grain is oriented along the zone axis. However, small tilts off zone axis often result in sharp contrast (due to phase contrast and/or high local densities of faults [72]) within grains, as typified in Figure 6a. Electron diffraction of the bottom regions of the grain also establishes the presence of residual beta phase, and imaging shows the same twins and stacking faults reside at identical locations in each beta region.

Although any particular section of a TEM sample of this microstructure exhibits the majority of the plate-like grains as being cross-sectioned at an oblique angle, the dark (diffracting) grain in Figure 6b is specifically oriented along the [0001] zone axis. This BF image at normal incidence presents the irregular shape of a typical plate-like grain. As the plate-like grain grows radially outward, it quickly impinges upon other growing alpha grains. Typically it cannot consume many of these grains, and thus begins to grow around them, thereby developing an interlocking nature. Figure 8 presents a plate-like grain cross-sectioned perpendicular to the [$\bar{2}110$] zone axis, which exhibits the multiple interlocking that can result from the development of plates with a high aspect ratio. (This interlocking and its positive influence on mechanical properties are further discussed elsewhere [66, 72, 106].) Also the irregular radial growth of these plate-like grains helps to envision how a plate-like microstructure produces a dense microstructure. Many of the apparent smaller grains imaged in any given section (Figures 6a and 6b) actually represent sectioning through outer extremities of large plate-like forms.

Ceramic materials typically incorporate impurities to aid sintering, and polycrystalline SiC materials processed below 2000°C often incorporate up to 20% secondary phases resulting from these additions. This ABC-SiC uses minimal additives; however, an assessment of how this microstructure develops without understanding the roles of secondary phases can be misleading. Experimental results detailing the secondary phases which form in ABC-SiC have been presented in earlier reports [66, 67, 72-74, 105], with only a summary provided here. The secondary phases have been categorized according to three geometries [72]. On the smallest scale is the presence of an amorphous grain boundary (Figure 5b) which is a residual by-product of the liquid-phase sintering process and the native oxide originally on each powder. Thin amorphous grain boundaries and small amorphous triple points contain primarily aluminum and oxygen, as determined by Auger Electron Spectroscopy of intergranular fracture surfaces [66, 73] and PEELS and EDS of TEM samples [69]. At the other extreme are large secondary phases which wet in amongst numerous matrix grains [66-68, 74]. These often reside in pockets where the original Al additive powder existed, and are less prevalent than in other *in situ* toughened SiC [45-53] and Si_3N_4 [76, 77] ceramics. Three crystalline phases have been observed in

these larger triple points; $Al_8B_4C_7$, Al_4O_4C, and Al_2O_3. The intermediate size is defined as "isolated triple points", which lie as triangular tubes on the planar surfaces of the plate-like alpha grains [105]. The box in Figure 7a and arrow in Figure 5a locate two of many triple points on the top surface of a plate-like grain, all of which exhibit similar diffraction contrast to the oriented SiC grain. Figure 7c presents a high resolution image that determines the presence of an orientation relationship between these crystalline triple points and their matrix grains, in this case:

$$[0\bar{1}1]Al_4O_4C \,//\, [0\bar{1}10]\alpha\text{–}4H \quad \text{and} \quad (100)Al_4O_4C \,//\, (0001)\alpha\text{–}4H.$$

These isolated triple points deflect cracks propagating along the grain boundary and consequently appear to affect toughness at the nanometric scale [72, 105, 106]. For the present study, the crystalline nature of these regions is believed not to affect the transformation process. Since the transformation is enhanced by the liquid-phase, it is important these regions of secondary phases be liquid during the transformation process. The crystalline ternary phases that form have melting temperatures above the lower processing temperatures; T_{melt} of Al_4O_4C is >2000°C, and T_{melt} of $Al_8B_4C_7$ is >1800°C [107, 108]. However, if these phases became crystalline during the SiC transformation, they would be expected to inhibit planar growth of the alpha top of the grain. Precipitates of these ternary phases are not observed trapped within the growing SiC grains, as has been observed for other secondary phases that are crystalline during the SiC transformation [109]. Thus these regions are believed to be liquid during processing due to the dissolution of SiC into the Al-containing liquid [107, 108] and the presence of other impurities [73], and these regions only crystallize upon subsequent cooling.

The processing temperature range evoked in this study of ABC-SiC extends over the range of the phase transformation from cubic (3C) SiC to hexagonal (4H) SiC. When processed at lower temperatures (below 1700°C), the densified material retained the beta SiC phase of the starting powders; whereas the materials processed at the highest temperatures (above 1900°C) were fully transformed to the 4H-alpha phase. Intermediate temperatures and short pressing times resulted in partially transformed microstructures. Figure 9 presents schematics of the densification, grain growth, and transformation in ABC-SiC. XRD and TEM couple to provide an assessment of changes in the crystal structure(s), whereas SEM and TEM couple to provide an understanding of changes in grain shape. HR-TEM and electron diffraction characterize the internal structure of grains and elucidate the transformation mechanisms. Additionally, SEM, TEM, and the widths of the XRD peaks all determine grain growth is substantial, both for beta grains at the lower temperatures and alpha grains at the higher temperatures. Thus the combined analyses of XRD, SEM, bright field TEM imaging, electron diffraction, and high resolution imaging are all necessary for an adequate interpretation of developing microstructure in SiC.

DISCUSSION OF TRANSFORMATION

The β–cubic to α–hexagonal phase transformation in polycrystalline SiC is a well-accepted phenomenon and is documented for the β–3C to α–4H transformation in ABC-SiC as a function of processing temperature in the preceding TEM results. With the renewed interest in SiC arising out of the ability to substantially improve the fracture toughness by developing an "elongated" microstructure, the ability to develop a reliable and reproducible processing scheme requires a well-understood analysis of the microstructure including the use of TEM. This change in crystal structure can correlate with a change in the shape of the grains, but this is not a necessity. Historically, the transformation to alpha, plate-like grains has been undesirable, because the transformation hinders densification and consequently yields poor mechanical properties [6]. However, it has become evident that an elongated grain structure can be beneficial, in conjunction with a fracture path around these grains, in a fully dense material [66]. Analyses of SiC microstructures, as well as processing conditions to produce these structures, are as varied as the many groups reporting on these materials. A sampling of different processing/results having been reported for polycrystalline SiC are listed in Table II. Since the fracture path can be influenced by the shape of the grains, mechanical properties appear to correlate better with SEM observations than with XRD data [66]. It is apparent that some SiC microstructures take advantage of a β–cubic to α–hexagonal transformation to develop this elongated microstructure. However, some microstructures develop a large volume fraction of elongated grains with a corresponding assessment of the ceramic retaining its β–cubic structure [61, 62]; and others exhibit an elongated microstructure developing from a mixture of α–hexagonal powders without detecting any phase transformation [56, 91]. Ideally, observation of the grain morphology would suffice as an analysis of the crystal structure, with β–cubic grains being equiaxed and α–hexagonal grains being elongated, as in other ceramics [76]. However, this morphology / structure correlation is not always simple in SiC. For example, the commercially available Hexoloy SA exhibits an equiaxed, fault-free, hexagonal microstructure [65, 69, 73].

Although the work of Heuer *et al.* [8-11] is often cited for a mechanism for the cubic-to hexagonal transformation in SiC, many recent processing results have produced microstructures that do not appear to obey this mechanism. The Heuer model has the alpha grain encapsulated in a sheath of beta phase with the β–to–α transformation occurring by passage of partial dislocations. (More details of the Heuer model are discussed in section *viii.*) The mechanism by which the present ABC-SiC transforms from β–3C to α–4H is dominated by a grain growth mechanism, rather than a traditional nucleation followed by growth, and without a necessity for motion of partial dislocations. In essence, a beta grain acts as a "seed" onto which the alpha grain grows. The alpha grain grows in a manner akin to Ostwald ripening and strongly influenced by interface attachment kinetics in a 1 nm-thick, liquid-phase medium. Only for the very last portion of the transformation (and at high temperatures) may reordering of stacking arrangements occur, which would necessarily entail motion of partial dislocations; and this stage may be preempted by subsequent transformations of the α–4H phase to other hexagonal

polytype(s). Furthermore, in this description of the cubic-to-hexagonal phase transformation, it is the intention to present a capacious mechanism that may correlate this transformation with the developing microstructures having been recently reported by others.

TABLE II

Starting Powders	Final Microstructure	Transformation?	References
a) beta	not elongated	no	20, 31, 37, 38, 47, 50, 54, 94
b) beta	elongated	no	61, 62
c) beta	not elongated	yes	32, 112
d) beta	elongated	yes	6, 8-12, 23-24, 28-30, 46, 49-51, 60, 91, 103
e) beta , <1% α–seed	elongated	yes	23, 37, 47, 48, 51, 52, 55
f) beta , <1% α–seed	not elongated	no	8, 11, 37
g) alpha	elongated	no	56, 91
h) alpha	not elongated	no	6, 20, 30, 40, 45, 46, 92, 133
i) alpha , <1% α–seed	not elongated	no	91, 63

i) Limitations of XRD Analyses of SiC

X-ray Diffraction can provide a qualitative appraisal of volume fraction transformed vs. temperature (Figure 1f and [23]); however, quantitative XRD of SiC is difficult due to irregular grain shapes and non-uniform distributions of faults and phases within each grain [57]. Most of the afore-cited studies (Table I) use no more than XRD to analyze the SiC structure, which can result in misleading assessments of the structure(s) and transformation(s). Accompanying this liberal utilization of XRD to characterize the phase transformations in SiC, numerous methods to quantify XRD analyses of SiC have been reported [4, 15, 23, 95, 100, 104, 110-113]. Whereas the present XRD analysis of ABC-SiC [66] and Ruska *et al.* [95] utilized six major peaks to perform a least squares fit of the experimental data to calculated patterns, Frevel *et al.* [104] modified the analysis to incorporate minor peaks. Yet Frevel *et al.* [104] concluded that the analyses of small volume fractions of mixed polytypes are subject to errors, even after assuming "a low degree of stacking faults" and "isotropic particles". More recently, attempts have been made to quantify stacking fault densities in β–SiC powders [112, 113]. Pujar and Cawley [113] concluded that experimental XRD of SiC indicates an irregular distribution of faulted regions or the presence of "two types of beta powders". Although the assessments were made that stacking fault density is reduced with annealing [112] and stacking faults are typically parallel within any one grain [113], these analyses do not account for grain growth, grain shapes, and the particular distribution of two polytypes within each grain that is observed in ABC-SiC by TEM.

Although small volume fractions of α–6H may be discernible in a judiciously prepared XRD sample of either a β–3C or a defect-free α–4H matrix, the detection of 6H (or a third polytype) becomes less sensitive in polycrystalline materials which contain a mixture of 3C and 4H phases. Furthermore, the propensity for stacking fault formation in SiC results in a relative reduction in peak intensities for all non-basal planes, thereby suggesting the material has a cubic structure. Stacking faults within one grain are all parallel to the basal plane, and often multiple phases may be stacked upon one another within one grain. The presence of parallel faults in cubic grains substantially reduces the intensity of three of the four $\{\bar{1}11\}$-type planes, thereby reducing the total intensity of the (111) peak. However, in hexagonal grains and/or dual-phase grains these parallel faults and polytypes provide constructive intensity to the diffraction peak representing the basal planes, (111) or (000z), where z = repeat number of the hexagonal polytype. The basal plane has the same d-spacing of 0.25 nm for all polytypes, including the cubic phase. Planes at an oblique angle to the basal planes, such as $\{0\bar{1}1n\}$, will have their XRD peaks "flattened" when closely-spaced stacking faults effectively reduce the crystallite size to a few nanometers [57]. The $\{0\bar{1}10\}$ sets of planes, which are normal to the basal planes, are typically used for distinguishing which polytype is present. (Note that the $\{0\bar{1}10\}$ peak is not present in all hexagonal polytypes; for example, it is absent in the 6H structure.) The other set of normal, low-index planes, $\{\bar{2}110\}$, have the same d-spacing for all hexagonal polytypes and also are indistinguishable from the {211} cubic planes. When larger grains and/or more widely spaced stacking faults exist, the relative peak

intensities for the $\{0\bar{1}10\}$ peaks of different polytypes enable the relative volume fraction of the different polytypes to be calculated. However, when the two phases coexist within the same grains with a small spacing between fault boundaries, these different $\{0\bar{1}10\}$ planes physically have a very narrow width. X-rays diffracting from nearby planes in the two phases destructively interfere with each other, which causes the $\{0\bar{1}10\}$ peaks for both structures to be substantially reduced. Since the stable polytype and the sequence of hexagonal transformations both depend strongly on the sintering additives, it becomes possible for various different processing schemes to produce multiple hexagonal phases, which in turn provide XRD patterns that erroneously suggest the cubic phase is the major phase.

Based on the recent XRD simulations [112, 113], the change in width of the (111) peak after densification (Figure 1a versus 1b) could represent a substantial decrease in stacking fault density. However, microstructural evidence in ABC-SiC suggests grain growth influences peak width, especially in light of these processed ceramics starting with a large number of very small (<20 nm) powders. Grain growth is expected to produce a reduction in total stacking fault density, as the regions of new growth at higher temperatures contain less faults. TEM, however, indicated the most significant reduction in this stacking fault density in β–SiC occurred as grains grew from 1700°C to 1780°C (Figures 3a and 4a), and not for the growth during densification. The more dramatic narrowing of the (111) peak occurs before 1700°C, in conjunction with grain growth during densification (Figures 1a through 1c). Moreover, the elongation of β–SiC grains with all faults parallel helps reinforce the (111) peak and reduce its broadening relative to all other XRD peaks.

Because of the difficult interpretation of peak intensities resulting from SiC with multiple phases present and a high density of stacking faults, XRD alone can not be used to establish the structure(s) present. TEM including both electron diffraction and high resolution, help establish the arrangement of the polytypes that are present within the ABC-SiC grains. Still, XRD provides an important statistical and qualitative analysis of the transformation(s), as presented in Figure 1f and [23], because of its ability to sample a substantially larger volume fraction of material [57, 6].

ii) Initial Growth of Beta Grains

The cubic-to-hexagonal transformation in polycrystalline SiC does not occur from a "static" beta microstructure, thus the dynamic changes transpiring as powders densify must first be considered. SEM and TEM imaging of the SiC hot pressed at 1700°C (Figure 3a) exhibit a microstructure comprised of beta grains with the average grain substantially larger than that of the initial SiC powders, as a result of grain growth incurred during densification. This is consistent with the qualitative reduction in peak width of the XRD peaks (Figure 1a vs. Figure 1b); having acknowledged that the relative XRD peak intensities and shapes are also sensitive to stacking fault densities, types of stacking faults, local distribution of stacking faults within the growing grain, shape of

grain, volume fraction of transformation, local distribution of transforming phase(s) within a grain, etc. [15, 57, 104, 113]. Since the transformation to the alpha hexagonal structure requires a temperature higher than 1700°C, the continued growth of these beta grains at the higher temperatures must also be considered.

Beta grains grow with a subtle elongation, with a planar top grain boundary that appears plate-like in shape when viewed by SEM (Figure 2a). The same single set of parallel (111) stacking faults (and microtwins) are evident in the growing beta grains, as were present in the starting powders. This single set of planar faults provides the beta grain with a top grain boundary having an energy lower than other grain boundary facets. (The low energy surfaces in these covalent ceramics are not dictated by the "most close-packed" plane, but rather by the number of terminated bonds. This bond termination is further complexed by the adsorbate from the surrounding liquid phase and its influence on surface reconstruction [114, 115] of the grain facet.) The other $\{\bar{1}11\}$ type surfaces of this grain do not have the same overall low energy as they are repeatedly interrupted by the impinging (111) faults. Since these $\{\bar{1}11\}$ type surfaces cannot develop large flat facets, the sides of the beta grains are irregular. For ABC-SiC these beta grains with a flat top and irregular sides develop because the original beta powder had been produced with 1 set of parallel stacking faults; however, similar grain shapes with parallel faults have been observed for "different" starting beta powders [8-11, 61, 91, 103].

When a grain grows parallel to the planes of stacking faults, the impinging faults provide many steps at the sides which simplify the growth attachment kinetics. For a beta grain to grow perpendicular to the planes of stacking faults, however, a new (111) layer must be nucleated. Since a thin liquid phase is present to enhance grain boundary diffusion, this layer-by-layer growth will be similar to the terrace-ledge-kink (TLK) model for crystal growth [116, 117]. Growth of SiC single crystals has historically [2, 6, 14, 118, 119, 120] been attributed to growth about screw dislocations [121], and vertical faults (perpendicular to the (111) growth plane) will form in single crystals when regions of growth around two screw dislocations impinge [119]. However, the lack of vertical faults (and partial dislocations terminating basal faults) in the middle of the small grains of ABC-SiC propound a TLK mechanism limited by nucleation is active for growth of these plate-like grains. Growth of a crystal about a screw dislocation usually makes for an "easy" growth direction, as new terraces need not be nucleated; and the growing crystal will typically retain the same crystal structure without additional faulting [14]. A TLK mechanism simplifies the formation of new stacking faults that are commonly incorporated during grain growth. The difficulty associated with nucleating each new terrace (as a "pillbox") on (111) planes makes growth perpendicular to the top (111) plane occur more slowly than growth parallel to the (111) surface. Thus the presence of one set of parallel faults, although in a grain of cubic symmetry, results in a grain with anisotropic boundary energies, and an anisotropic growth morphology.

When a new layer of the β–SiC is nucleated on the (111) plane, it is often possible for the layer to develop the wrong stacking arrangement for 1 or more layers, thereby producing stacking faults and/or microtwins. Because the energy of a stacking fault is minimal, they are common in most SiC materials at all temperatures. In this study, TEM imaging did not resolve any significant difference in the stacking fault density in the β–3C grains as a function of temperature, from 1600°C to ~1700°C; however, a qualitative reduction

in stacking fault density occurred in the beta grains grown at 1780°C for one hour. The beta grains processed at 1700°C exhibited a random spacing of stacking faults and twins throughout the thickness of the grain, whereas at 1780°C the stacking fault and/or microtwins exhibited a larger spacing near the tops of grains as compared to the bottom. The rationale in this variation in stacking fault density across the thickness of the grain appears to relate to the lower portion of the grain starting to grow while heating, with the nucleation of stacking faults more common at the lower temperature. Subsequent upward growth of the grain at higher temperatures correlates with a reduction in stacking fault density. A recent study [112] has discussed quantitative analysis of stacking fault densities by XRD, and indicated such differences can affect the developing microstructure; however, such analyses, without support from TEM data, may be subject to inconsistent results since the stacking fault density varies through the thickness of the grain. Annealing SiC is claimed [112] to reduce stacking fault density (i.e. implying they anneal out by motion of partial dislocations). However, if during this anneal the grain size is changing, the new regions of grains which grow perpendicular to the faults may be expected to grow with a lower fault density. This would reduce the total stacking fault density without the need of having any stacking faults within a grain be moved by partial dislocations. In single (large) crystals, however, reduction of stacking fault density must eventually (or at high temperature) be by motion of partial dislocations, as grain growth is not viable.

Once a faulted layer is nucleated on the (111) plane, it readily grows to the radial extremes of the grain; i.e. stacking faults almost always end at the grain boundary, and no partial dislocations in the middle of a grain were observed in these ABC-SiC's processed below 1900°C. (A few initial beta powders exhibited nonparallel twins, which necessarily intersect at partial dislocations; however, these grains became less prevalent after sintering.) The stacking faults terminating at the grain boundary produce steps of close proximity, which not only prevent the development of large facets on the $\{\bar{1}11\}$ surfaces, but also inhibit the nucleation of stacking faults on these $\{\bar{1}11\}$ planes. Furthermore, since the (111) stacking faults are not terminated by partial dislocations in the middle of the grain and the driving force (energy to be gained) is minimal to remove a full-length stacking fault, it becomes difficult to "anneal out" stacking faults. Thus those stacking faults (and microtwins) grown into a beta grain at lower temperature are not removed as the grain continues growing at higher temperatures. This hindrance to motion of stacking faults persists even at the higher temperatures where transformation to the alpha phase occurs (discussed further in section *v*).

Whereas the shapes of the smaller beta-SiC grains in the microstructure processed at 1700°C and 1780°C are primarily a function of the shapes of the initial powders, the shapes of the larger grains provide an indication of how beta-SiC grows. After one hour above 1700°C, these larger grains are typically less than 1-2 microns in size and have a nominal aspect ratio of two [44, 66]. The presence of only one set of (111) stacking faults causes the beta grain to incur anisotropic growth. As the grain gets bigger, however, the regions of $\{\bar{1}11\}$ facets between impinging (111) stacking faults become larger (especially in the third dimension). Since these regions have the same energy as the top (111) surface, the anisotropic growth becomes limited, and the beta-cubic grains do not develop higher aspect ratios. It is noted that hexagonal α–6H microstructures

exhibit equiaxed grain shapes, such as in Hexoloy SA, when few stacking faults are present [6, 73]. Thus the steps in a grain boundary facet, caused by impinging, closely-spaced stacking faults, can strongly alter the grain boundary energies, which in turn affect the morphologies of SiC grains.

iii) Stacking of Planes Converts to Alpha Phase

Since each new basal (111) layer nucleates without a strong dependence on the subsurface layers (i.e. stacking faults are easy to produce), there becomes a temperature (or range of temperatures) when the stacking arrangement converts to that of the thermodynamically favored alpha phase (possibly dependent on the presence of impurities). Since the stacking faults are also common in the α–4H material, this conversion in the stacking sequence does not occur at one discrete plane. Nor does this transformation occur at a discrete time and temperature in all grains. Furthermore, the transformation temperature, as well as the transformation product, can be influenced by the particular sintering additives used [28, 42, 43].

ABC-SiC materials hot pressed above 1700°C all exhibit (Figures 4a, 5a, and 7a) a "conversion" in stacking from the β–3C to α–4H as the grains grow. Since the transition in stacking is not a discrete interface, but rather exhibits a mixed region of beta and alpha, there appears to be a critical nucleus (or thickness) of α–4H phase necessary before all growth continues as the α–4H phase. The transition zone appears thinner for the materials hot pressed at higher temperatures, implying this phase conversion can occur during the heating process. Similarly, the transition zone appears at a lower location in the grains processed at higher temperatures, again because less time for growth was incurred before the temperature became sufficient for the stacking sequence to become fully α–4H. Thus longer times at higher temperatures result in a larger fraction of alpha phase in each dual-phase grain. The conversion in stacking, and the subsequent development of the alpha top of the grain, proceeds as a grain growth process, with Si and C atoms arriving at a growing grain via the 1 nm-thick liquid medium. New basal layers of the α–4H appear to nucleate in the same TLK manner [117] by which the beta phase was growing.

Again vertical faults (perpendicular to the basal planes) are not typically observed in the α–4H regions. If terraces nucleate as "pillboxes" [117], the nucleation of two α–4H regions at different locations, with different stacking sequences, would be expected to generate vertical faults such as the DPB's (Double Position Boundaries) observed in 3C layers epitaxially grown on 6H or 15R substrates [122, 123, 124]. Since stacking faults are common in SiC, nucleation of two "pillboxes" per basal layer would also make vertical faults more common. The other possible growth mechanism in SiC, about screw dislocations, would hinder the conversion of the stacking sequence from β–3C to α–4H. Furthermore, the presence of two screw dislocations per grain would also be expected to result in the formation of vertical faults. The occasional steps in the planar top α–4H grain boundary (Figure 5b) are often 4 atomic planes high, which is equivalent to the ~1 nm Burgers vector expected for growth about a screw dislocation [14, 121]. However,

STM of CVD growth on vicinal a-6H single crystals without screw dislocations has also observed "step-bunching" equivalent to the polytype stacking [115]. The growth of the α–4H grain into a plate-like shape (to be discussed in section *iv*) supports the "pillbox" and TLK nucleation, as growth about screw dislocations often promotes the formation of whiskers or needles [3, 121]. Whichever growth mechanism exists, pillbox nucleation or screw dislocation, the addition of each new terrace is the rate limiting step. Once nucleated, a basal layer quickly grows to the horizontal extremes of the plate before a second nucleation event occurs, precluding the development of vertical faults. This single nucleation event per basal layer dominates over a wide range of grain sizes, from submicron beta grains to alpha plate-like grains >10 microns in diameter, and a variety of processing conditions. As grains become larger (and/or processing temperatures more severe), second nucleation events and vertical faults should become more probable.

The Al additive, which becomes a liquid-phase (or glassy phase) sintering aid during hot pressing, appears to encourage the changeover to the α–4H stacking at a temperature well below 1900°C. However, it is not clear whether the Al plays a kinetic or a chemical thermodynamic role. Several research articles have noted the influence of Al and/or Al_2O_3 additive on promoting α–4H formation, as well as lowering the transformation temperature [23-26, 28, 49, 51, 52, 80]. Tajima and Kingery [39] used XRD to determine the solubility of Al in α–4H SiC as 0.26 wt. % and 0.5 wt. % at 1800°C and 2000°C, respectively. (In their work, excess Al was "burnt off" to prevent the formation of secondary phases; however, TEM was not conducted to detect Al-based ternary phases.) Mitomo *et al.* [80] detect ~0.4% Al in α–4H processed 8 hr at 2000°C and <0.1% Al in α–6H after processing 8 hr at 2400°C. (Again no TEM analysis discusses where the Al resides nor where it goes upon annealing.) Shinozaki *et al.* [52] report that EDS-TEM determines 0.8 wt % Al is in the α–4H grains, with an enrichment at the ends of the plate-like grains; however, analyses of the present ABC-SiC by PEELS, Auger, and HR-TEM indicate the Al at edges of grains is due to triple point phases and amorphous grain boundary layers [69, 72, 73, 105]. EDS-TEM analysis of these ABC-SiC plate-like grains indicate a trace (<1 atomic %) Al is present throughout the α–4H regions, but attempts to establish a chemical difference between the alpha and beta portions of the dual-phase grains has thus far been inconclusive. (Recent EDS investigations of grains comprised of both α–4H and α–6H regions also resolved no differences in the Al content of the two hexagonal phases [109].) The residual Al-containing secondary phases, even when only 1% Al is added to ABC-SiC, suggest minimal Al is incorporated in the α–4H. If the inclusion of Al is necessary to invoke the α–4H stacking sequence, the "conversion" regions may be expected to be more discrete, as they would represent growth at a time and place when the amount of free Al available were highest. In fact, continued growth of α–4H grains could consume sufficient Al, such that subsequent growth reverted to the β–3C stacking. No beta is observed at the tops of plate-like grains, even those processed to the largest grain sizes. Conversely, if β–3C is a stable low temperature phase, then (slowed) growth during cooling from the processing temperature should cause the top few planes of each plate-like grain to be comprised of β–3C. Although the tops of plate-like grains are always α-4H (Figure 5b), stacking faults are often present in these top layers, and this may represent an "attempt" to grow β–3C phase

as the temperature lowers. The question of phase stability as a function of temperature and impurity concentration remains unanswered (section *ix*).

In this study of ABC-SiC, both the transformation and densification are retarded when only 1% Al is used as a sintering additive (Figure 1f) [26, 66, 72]. It is believed this chemical effect represents insufficient Al to react-away the native oxide on SiC powders, thereby preventing grain growth and consequently preventing α–4H formation. Thus it is possible that Al does not play a necessary chemical role to invoke the α–4H stacking. Rather, the Al-based liquid provides a mode by which transport of Si and C are enhanced (as well as removing native oxides from the SiC powders [93]), thereby enabling the stacking sequence to follow the thermodynamically predicted [17, 18] α–4H stacking sequence.

iv) 4H Grain Elongation & Shape Development

Once a critical nucleus (thickness) of α–4H has formed on top of the beta grain, the thermodynamically favored alpha portion of the grain will experience faster growth than the lower beta part of the grain, as well as faster than the other beta grains in the surrounding matrix. Furthermore, the larger anisotropy associated with the α–4H structure enhances the elongated growth of the alpha phase to develop plate-like grains with aspect ratios upwards of 10. The parallel faults within the α–4H phase also can enhance this anisotropic growth. However, since there is a lower density of faults in α–4H than was present in the beta phase, the higher aspect ratio in the alpha phase appears to be influenced by anisotropy in the structure more than by the parallel faults disrupting the ends of plate-like grains. (Another argument would say the anisotropy of the α–4H structure is due to its "natural" stacking faults on every other plane.) The non-basal facets of the α–4H allow for easy attachment kinetics; and coupled with the thermodynamic preference, the ends of the α–4H plates grow rapidly to consume the neighboring beta grains. The 1 nm-thick liquid phase along the grain boundary enhances the mobility of adsorbed states, thereby enabling the elongated growth to be defect free. Whenever a basal stacking fault has been incorporated in the α–4H stacking, it will be continuously propagated as the plate-like grain lengthens. Just as stacking faults of beta do not nucleate on the ends of the beta grains, neither do additional variants of α–4H nucleate on the ends. Kinsman and Shinozaki [103] also noted that alpha develops "along only one of the cubic close-packed plane variants in each grain."

Although not as prevalent as in the beta phase, stacking faults are common in the α–4H. The minimal additional energy due to a fault unfortunately means the driving force to remove a stacking fault is small. It is much easier to diffuse atoms through the 1 nm-thick liquid phase than to experience the "coordinated" motion necessary to nucleate a partial dislocation (most probably at a grain boundary) and move it to propagate a

stacking fault along a basal plane. Thus the growing alpha phase does not consume its lower beta-seed portion of the grain. In fact, the upper alpha portion of the grain views its lower beta half as planes of stacking faults. When the alpha portion elongates, it pulls the lower planes of beta stacking along with it, thereby ensuring continued dual-phase growth. The growth of the beta portion appears to lag behind the top alpha phase, thereby giving the grain an overall "bowl-like" shape (Figure 9c). Exceptions to this in each grain are the irregular facets (Figures 5a and 7a) in the lowest sections of the beta phase (discussed later in this section).

Many plate-like grains exhibit flat, faceted ends; however, these facets can be an illusion of the imaging conditions. For example, the diffracting plate-like grain in Figure 5a suggests it is terminated by the $(0\bar{1}10)$ plane. However, high resolution imaging of this facet determined this grain boundary is not parallel to the electron beam (for the $[\bar{2}100]$ zone axis imaging conditions of Figures 5a and 5b) and therefore not parallel to $(0\bar{1}10)$. The end of this plate appears straight because of its intersection with the basal surface of another plate. No preference for growth in $\langle\bar{2}110\rangle$, nor $\langle 0\bar{1}10\rangle$, directions are observed for these plate-like grains, as is reported for other hexagonal platelets [125]. The α–4H grains appear to grow uniformly in all radial directions, except where they impinge other grains (Figure 6b). (The effects of impinging grains on shape are discussed in the next section.) In general, the ends of plates processed at 1900°C exhibit these apparent facets (Figures 5a and 8); however, after processing at higher temperatures rounded ends are quite common (Figure 6a). The corners of facets (other than the top planar grain boundaries) formed at all temperatures, appear rounded as imaged by HR-TEM, presumably due to the surrounding Al-containing glassy phase(s).

The plate-like shapes of these dual-phase ABC-SiC grains are further compromised by the rough irregular facets observed on the bottom grain boundaries (Figures 4a, 5a, 7a, 8), which in turn enhance the mechanical integrity of this microstructure [69, 72]. These lower regions exhibit stacking indicative of beta phase, incorporating microtwins and numerous faults. Separated beta regions, such as imaged in the TEM sections of Figures 5a and 7a, exhibit faults at identical stacking locations in each region. This indicates that during growth these regions are actually connected outside the plane of the TEM section, and that these planes are propagated by elongated growth around the other alpha grains which impinge the bottom of this particular grain. As previously mentioned, beta planes are "pulled" along by the elongating top alpha portion of the grain. However, at certain locations the elongation of the beta planes is hindered, and they must grow around these "obstacles". Since the beta planes, like their parallel alpha planes above, grow by consuming surrounding beta grains, it is presumed that the local "obstacles" to growth are other grains, comprising the alpha phase, which arrived there first. In a particular section, such as in Figures 5a and 7a, these separated beta regions at the bottom of the plate-like grain exhibit facets that have angles between ~35° and 70° to the basal plane of the grain. These are the projected angles that other $\{\bar{1}11\}$-type planes make with this $[\bar{1}10]_{\beta\text{–}3C}$ orientation. Higher magnification images indicate facets between 35° and 70° are actually comprised of mixed $\{\bar{1}11\}$ facets. These beta facets indicate beta planes elongate in a sluggish manner that includes interface attachment but also sequential development of $\{\bar{1}11\}$-type facets. This is in contrast to the upper alpha basal planes

which grow in a relatively uniform radial manner, except where they impinge other alpha grains (Figure 6b). When beta growth is hindered by an "obstacle", a $\{\bar{1}11\}$-type facet develops, and continued elongation of the beta has to occur in another radial direction. After many turns around "obstacles" the beta planes elongate to the radial extent of the plate-like grain, but with the discontinuities evident in the irregular beta bottom in Figure 7a. Finally, each irregular region is truncated by a bottom-most (111) facet; and the lack of growth perpendicularly down from this bottom is discussed in section *ix*.

v) Later Stage of Transformation & Refinement of Grain Shape

Thus far only isolated growth of the dual-phase grain has been considered. The alpha portion gives this grain a thermodynamic advantage over the beta grains in the surrounding matrix. However, since the dominant macroscopic mechanism is grain growth akin to Ostwald ripening, surrounding beta grains are also trying to grow. Fortunately, once the alpha-containing grain gets bigger, the grain growth driving force further enhances the preferential growth of the dual-phase grain at the expense of its smaller neighboring beta grains. Yet, the final transformed ABC-SiC does not develop a duplex microstructure comprised of two distinct grain sizes, because other beta grains have developed alpha portions and have also grown into plate-like, dual-phase grains.

During this growth-controlled transformation, multiple plate-like grains begin to impinge each other, thereby impeding their uniform radial growth. Based on an aspect ratio upwards of 10, and microscopic analysis [69, 97], this impingement becomes significant at temperatures above 1780°C (for 1 hour), where the total volume fraction transformed remains well below 1/2. The end of an elongating grain, which impinges the flat top of a second plate, will have its growth in that radial direction truncated, resulting in the apparent facets (Figures 5a and 8) characterized in the previous section. However, the grain continues to elongate in other unimpeded radial directions (Figure 6a), eventually growing around other plate-like grains to develop the interlocked microstructure (Figures 2b, 8, and 9d). As the transformation continues, the increase in aspect ratio, coupled with the plate-like shape, result in an increase in interlocking of the grains. This interlocking in turn causes an increase in the strength of ABC-SiC even though the average grain size is increasing [66, 69, 72, 97]. Furthermore, these interlocked plates (coupled with an intergranular mode of fracture) can create elastic bridges [66, 69, 75] or "pins" [126, 127, 128] in the wake of an advancing crack tip, thereby increasing the fracture toughness.

A fully dense material comprised of "elongated" grains is typically envisioned to have a microstructure similar to that of gypsum or martensite in steel. Whether laths or needles are formed in a solid state transformation, the first transformed shapes grow large until they impinge each other. Subsequent transformation of material between these large elongated laths produces successively smaller laths until all of the material is comprised of laths of widely different sizes. However, the interlocking nature of growth in plate-like ABC-SiC complicates this microstructure, such that a typical two-dimensional representation is insufficient. The irregular shape of interlocked plates depicted in Figure

6b means that much of the space between impinging larger plates can be filled by the extremities of other large plate-like grains. Thus even the limited distribution of grain sizes suggested by Figures 6a and 9d is inflated, and many of the smaller grains correspond to sections through the outer extremities of larger plate-like grains. A few of the smallest grains, however, do represent small, less-plate-like grains, necessary to fill space. These smallest grains are identified as α–4H, implying they had transformed to alpha plate-like grains but were subsequently partially consumed by continued growth of other grains.

The last stages of the transformation can be incurred at sufficiently high temperatures such that the ends of the plate-like grains become rounded (Figures 6a and 6b). Although the alpha grain size continues to increase, it is also evident that the aspect ratio decreases [66, 89]. Other alpha phase SiC materials processed at higher temperatures have exhibited equiaxed microstructures [6, 20, 30, 40, 45, 46, 64, 65, 73, 92, 129]. As the alpha grains become less elongated and more rounded at the ends, the extent of interlocking is also reduced and mechanical properties deteriorate [89]. When ABC-SiC is processed at higher temperatures, more SiC is dissolved into the liquid phase [108]. The higher volume fraction of liquid at triple points will tend to cause corners of grains to become more rounded. Resolidification of SiC out of the liquid upon cooling may have insufficient kinetic mobility to redevelop the sharp corners in the SiC grains.

In addition to a change in grain shape, the ABC-SiC processed at 1950°C exhibits trace evidence of the formation of α–6H, as identified by both TEM and XRD. TEM observes a few grains with α–6H regions (and α–15R) in the middle of grains, and some of these α–6H regions are terminated by partial dislocations. This suggests the higher temperature is sufficient to invoke partial dislocation motion, and that subsequent transformations at higher temperatures (i.e. eventually to the equilibrium α–6H phase) can occur via the motion of stacking faults. Since the middle transition (from beta phase to alpha phase) zone has a high density of faults [72], it is expected that the dislocation-invoked transformation to the α–6H phase will be nucleated on these internal faults. With the grains having already grown many microns, the driving force for continued growth is lessened. Thus the more mobile partial dislocations at the higher temperature can become more influential than grain growth for subsequent transformations. The eventual removal of stacking faults within grains, either via transformation to α–6H or just as a consequence of high temperature annealing, removes one of the driving forces for shape anisotropy and encourages the development of equiaxed grains. Also the $\{\bar{1}102\}$ planes in the α–6H structure are similar to $\{\bar{1}11\}$-type planes in the cubic structure; thus a non-faulted α–6H grain is expected to be more isotropic in shape than is an α–4H crystal. (Morphologies observed by others are discussed in section *viii*.)

One question that arises is: "Why do beta regions persist at the bottom of the plates (Figure 7a) even as the transformation nears completion?" The previous section discussed why these irregular beta regions at the bottom of plates do not grow, but now it is considered that such beta regions could be consumed in one of two modes. The first would be in the transformation mode discussed in most other reports on SiC; that is by the passage of partial dislocations and stacking faults to allow the alpha phase to thicken

and grow "down" to consume the beta phase. Although this eventual consumption of beta will be incurred at sufficiently high temperatures, it does not easily occur because a grain's energy is negligibly reduced by removing the relatively low energy stacking faults. At the very later stages of transformation, the alpha phase may grow down in singular, full-plane increments, but it becomes hindered when it reaches the irregular bottom surface. For the alpha phase to continue consuming these beta regions would result in a rough bottom surface comprised of many regions of high energy (non-basal planes) facets of the hexagonal structure. These higher energy facets would leave the grain with more surface energy, so it prefers to keep the beta regions with their relatively lower-energy $\{\bar{1}11\}$ facets. The alpha basal planes growing down to consume the beta at the bottom of the grain could try to retain an atomically planar nature, but this would require them to consume other alpha plate-like grains between the beta regions (Figure 7a). This growth is a stalemate, because these other alpha grains are trying to grow "fast" in their elongating direction, while the first alpha plate is trying to keep its low energy basal face atomically flat.

The second mode would be the consumption of these beta regions by the numerous impinging elongated alpha grains on the bottom surface. These alpha grains were growing "fast" in their elongated direction, until they reached the low-energy alpha basal facet of the first grain (or even planar regions of beta at the bottom of the plate, such as in Figure 5a). For these impinging alpha grains to consume the intermediate beta regions between them (see Figure 7a) would require the impinging alpha grains to grow thicker. Thickening of alpha plates is slow, and if it occurs in this geometrical format, these impinging alpha plates would have to disrupt their atomically flat, top basal facets. This would produce rough facets on the top of each alpha plate, with higher energy than the $\{\bar{1}11\}$ facets of the beta it is trying to replace. Thus the beta regions persist.

vi) Competitive Grain Growth

For the processing conditions incurred by these ABC-SiC materials, densification, grain growth, and transformation are coupled; yet such is the typical case for polycrystalline SiC transformations reported in the literature. Since full densification is possible with the Al-B-C sintering additives by hot pressing at ~1650°C, it is believed that nearly all of the densification occurs prior to the majority of the transformation for the materials hot pressed above 1800°C. Thus it appears the transformation and grain growth can be considered after the densification is complete. The transformation of SiC is often reported to involve the motion of partial dislocations and stacking faults to bring about the phase transformation [5-16, 26-34, 45-56, 103]. Such a kinetic mechanism may be considered as in competition with the beta grain growth kinetics; and although both can occur simultaneously, typically the dominant mechanism is considered as "independent" of the other, as it will eventually control the process. Since the final product is a transformation to the alpha phase, the growth of the beta grains is often ignored in reports of the transformation. (Some works of others are detailed in the next section.)

However, the observed transformation in ABC-SiC exhibits an interaction with the beta grain growth that does not represent "real" competition. Rather this transformation depends on the grain growth, with a plot of grain size vs. processing [66] tracking that of volume fraction transformed (Figure 1f). Densification, grain growth, and beta-to-alpha transformation all have the same requirement, that atoms move along grain boundaries, and enhanced by a liquid-phase medium. Thus grain growth occurs when densification occurs, and the transformation to the thermodynamically-favored alpha phase occurs when grains grow. Even processing ABC-SiC at 1900°C (for 4 hours) provides insufficient thermal driving force to nucleate a partial dislocation, at a grain boundary, so that its passage through the crystal to produce a stacking fault can bring about the transformation. If stacking faults did not terminate at grain boundaries, but rather at partial dislocations in the middle of the grain, then the thermal energy need only be sufficient to move the dislocation and nucleate the alpha phase. In small grains, however, stacking faults are terminated at grain boundaries. On the other hand, 1700°C is sufficient temperature to incur some grain growth, especially if Al-containing additives provide a liquid medium for enhanced grain boundary diffusion.

Since some grain growth is incurred during densification, even at temperatures as low as 1600°C, it is expected that the transformation should occur, too. If enough time could be allocated at 1600°C to 1700°C, in order to incur sufficient grain growth, then growth of the alpha phase should eventually occur in the same manner as has been observed at higher temperatures. The minimal grain growth incurred at lower processing temperatures, however, is never sufficient to nucleate a critical alpha portion of a grain. Three possible reasons for the lack of transformation at 1600°C are proposed. First, it is possible that the β–3C phase is the equilibrium phase in the temperature range of 1600°C - 1700°C. This does not agree with theoretical calculations that β–SiC is always metastable [17, 18, 84, 85] nor with some experimental single crystal growth [82, 83]. Yet β–3C single crystals [81, 82, 129] and β–SiC thin films on planar α–6H single crystals [114, 115, 122, 123, 124] have been grown in the temperature range of 1500°C to 1900°C, when a supersaturation of Si exists. Secondly, it is possible that the β–3C phase is preferred for small crystals, where the multiple {111} facets lower the surface energy / volume ratio. This is consistent with the practical observation in the literature that starting β–SiC powders are usually submicron and starting α–SiC powders are commonly >1 micron, independent of whether initial preparation of powders is in the gas phase or via reaction in the solid state. (Rarely are starting powders critically characterized by TEM to establish whether multiple phases exist in each crystallite.) Whether β-3C is a thermodynamically stable phase over a limited temperature range or metastably grows due to chemistry and/or geometrical size, the (limited) growth of β-3C is commonly reported. Thirdly, the 1600°C temperature range is where the additives in ABC-SiC begin to crystallize. In the pseudo-ternary sections of phase diagrams [107, 108], the ternary $Al_8B_4C_7$ phase that results from these additives forms a liquid eutectic with SiC below 1800°C. The presence of other impurities, such as oxygen and sulfur [73], are expected to further lower the liquidus temperature. At lower temperatures where the eutectic reaction leads to crystallization of triple points, however, grain boundary diffusion through the amorphous phase at the boundary also becomes sufficiently impaired that both grain growth and the transformation are practically

stopped. The top planes of the plate-like SiC grain never grow past the interface (nor circuitous) of the crystalline triple point (Figures 5a, 7a, and 7c), neither as the α–4H phase nor as the β–3C phase.

The grain growth incurred in ABC-SiC, as well as the transformation dependent on it, involve two kinetic driving forces. Macroscopically, grain growth is incurred akin to Ostwald ripening. Beta grains grow at temperatures below 1700°C, and alpha grains are continuing to grow at temperatures above 1900°C. At intermediate temperatures the anisotropic growth of the plate-like grains at first suggests that interface attachment dominates the kinetics of the growth (and transformation) process. Interface attachment kinetics control both local motion of grain boundaries and stacking order of basal planes. The elongation of plate-like grains is controlled by the atomic interface attachment. But a fast growing grain will be stopped once it reaches a flat basal facet of another plate-like grain. This is repeatedly observed by TEM as a stalemate in growth of these two grains. Still, observations determine grains continue to grow, and the driving forces akin to Ostwald ripening remain macroscopically dominant.

At the nanometric scale, interface kinetics do control how a grain boundary moves. A grain elongates by depleting SiC from the liquid phase. This in turn develops a concentration gradient across the liquid phase, which causes SiC to be dissolved off a neighboring grain that is to be consumed. However, an elongating grain is stopped when it impinges the planar surface of a second alpha grain, even when the second grain is smaller than the first. The desire to develop low energy facets is predominant. The nanometer-thick liquid phase between grains facilitates the dynamic interactions involved in grain boundary motion, but once a stalemated interface has developed, the net flow across the boundary becomes minimal. Additionally, the impurities within the liquid phase may be expected to terminate grain boundary facets, further lowering their energy. The liquid phase sintering alters the activation energies, but does not change the interface attachment mechanism. Similarly, the liquid phase enhances grain boundary diffusion to make grains grow faster, but the macroscopic mechanism of growth (and transformation) remain akin to Ostwald ripening. For a growth-induced transformation, when grain growth is prevented, the transformation does not occur, as shall be discussed in the "unanswered questions" section.

vii) Transformation Based on Beta Grain as a Seed

The processing of SiC to develop a desirable microstructure is often incurred through the use of seeds, with a few seed grains growing to consume all the matrix grains. The present β–to–α transformation in ABC-SiC can be thought of in terms of a "seed" process even though no seeds are intentionally added. In terms of classic crystal growth, the beta grain acts as a seed onto which the large alpha grain grows, without the beta seed itself being consumed. The dual-phase grain that develops from this growth on the seed is observed in the early (Figure 4a) and latest (Figure 7a) stages of the transformation. In fact, all beta grains in the surrounding matrix are quickly consumed by the growth of the

plate-like alpha grain, while the beta seed portion of the growing grain remains until the end of the transformation. Although numerous beta regions persist at the bottom of a sectioned grain (Figure 7a), only one (or none in an average TEM section) represents the original beta seed. Apparently, the passage of partial dislocations to transform the beta region(s) into alpha phase provides an energetically unfavorable mechanism at the temperatures incurred for transformation in ABC-SiC. In a common solid-state transformation theory, a defect often acts as the seed for nucleation, and growth is typically radially outward (sometimes star-like or dendritic in nature). But in such a case, the seed is consumed, as the removal of the defect energy becomes a kinetic driving force for the transformation. The energy of stacking faults in SiC, and regions of beta in an alpha grain can be considered as such, cause minimal excess energy, and therefore provide little driving force for their removal. Although the α–4H grain exhibits a strong two-dimensional radial growth, growth in the third dimension is slow and limited to only upwards away from the seed, similar to a classic crystal growth from a liquid medium [117].

viii) Comparison to Results of Others

A wealth of literature discusses the beta-to-alpha transformation in SiC; however, none describes the transformation to be a consequence of grain growth, as presented for this ABC-SiC. And yet reported transformation data in polycrystalline SiC typically presents evidence of grain growth. A quantitative analysis of the phase transformation can not be conducted without the incorporation of multiple techniques [6], and misinterpretation of data is relatively easy in these complex, faulted microstructures. It is the intention of this discussion to consider that data presented for other polycrystalline transformations mechanisms can be consistent with the mechanism observed in ABC-SiC. To that end, the dislocation-induced transformation in single (large) crystals is briefly reviewed; reported TEM data is compared to images acquired for ABC-SiC; and grain morphologies presented in metallographic analyses and XRD data are reviewed in light of what has been observed for ABC-SiC.

The numerous reports on crystallography, mechanical properties, and semiconductor properties, which also involve transformations (and growth) in SiC, provide an extensive range of data that appears difficult to place all within one transformation mechanism. Three mechanisms have been discussed in the literature; a mechanism by which partial dislocations move to create stacking faults which in turn produce a change in the stacking arrangement [4-7, 15], a theory where grains are "vaporized" and "recrystallized" as a new phase [1-3, 15], and a processing scheme whereby a small volume fraction of seed grains of a favorable crystal structure grow to consume the surrounding matrix [2, 6, 8-11, 47, 48, 54-56]. The growth of seeds may clearly dominate the transformation in polycrystalline SiC. In fact, unidentified traces of different "seed" polytypes have been blamed [7] for the "wide range of experimental inconsistencies in SiC transformation". Also it is clear that the classic "FCC to HCP" transformation [130, 131, 132] by

introduction of stacking faults, and motion of partial dislocations, is a dominant mechanism in single crystals [6, 7], where grain growth cannot play a role. However, the "vaporization and recrystallization" theory has been discounted, as not being a valid "solid-state transformation mechanism" [4, 6]. Instead it is typically accepted that the transformation via stacking faults and partial dislocations not only controls the single crystal transformation, but also controls the transformation within each grain of a polycrystalline matrix.

Historically, the "vaporization and recrystallization" mechanism could be accepted because; (a) single crystals were commonly microscopic in size and decomposed followed by recrystallization via the vapor state [3], and (b) polycrystalline SiC was never dense, thereby providing 10-40% internal porosity for vapor transport. Even in modern polycrystalline SiC with >5% porosity, vapor transport must be considered viable. Many processing schemes can have the beginning of the phase transformation precede full densification of sintered SiC materials, again allowing for possible vapor transport. The vaporization and recrystallization mechanism has been extended to consider transport though a liquid [6], but even there it has been believed that the initial nuclei of alpha phase must form via a solid state mechanism, such as motion of partial dislocations. Mechanisms involving either vapor and/or liquid transport have been classified as not "solid state transformations" [6]. Therefore the mechanism observed in ABC-SiC would not be considered a solid state transformation because of the enhanced diffusion through the grain boundary phase. Yet, it is doubtful that a fully-dense, polycrystalline SiC can be produced without a 1 nm grain boundary phase. SiC powders have a native oxide which must be removed, typically via reaction(s) with sintering additives and/or processing environments, in order to be sintered. If the aids fully "deoxidize" the grain boundary, an impurity layer persists [76, 133]; however, in ABC-SiC [66, 69, 73] oxygen remains in the grain boundary phase. For an ideally pure SiC, densification is still easier by diffusion along grain boundaries. Grain growth in SiC is also enhanced by diffusion along grain boundaries, at which typically resides impurities and residual oxide. Although the grain growth and the growth-induced transformation in ABC-SiC may not be considered as "solid state" because of the enhanced kinetics caused by a ~1 nm-thick amorphous grain boundary phase, this β–3C to α–4H transformation can and does occur in a dense, solid material.

Based on HR-TEM research to investigate single crystals and epitaxial films of SiC, the passage of partial dislocations can invoke the cubic-to-hexagonal transformation [6, 7, 12]. Pirouz *et al.* [7] present a model where a cross-slipping screw dislocation leaves partial dislocations and faulted loops on the basal planes in its wake. Three of six planes incur faulted loops to change the stacking from ABCABC to ABCACB; and the model is easily altered to justify the 3C to 4H transformation. Although this requires less activation energy than nucleating independent partial dislocations on each plane, this model still requires "a dislocation source" [7]. Powell and Will [134] noted that roughening the surfaces of metastable α–2H single crystals resulted in a phase transformation occurring more than 1000°C lower than unscratched crystals. On the other hand, Inomata *et al.* [21] had pure, fault-free beta single crystals that did not transform after prolonged annealing at 2300°C. Both of these results are consistent with

transformation in single crystals due to partial dislocation motion, but also with an energetic difficulty to nucleate partial dislocations.

The introduction of a planar fault into a crystal, whether to create a stacking fault or a twin, is commonly presented in materials textbooks [135] as energetically easier by moving a partial dislocation, Thus the many fault-based transformation mechanisms in SiC, whether based on twinning [10, 12, 13] or stacking faults [4, 112], are in turn probably dependent on a dislocation mechanism such as that of Pirouz [7]. Pandy and Krishna [5] present a "basal shear" mechanism which requires "diffusional rearrangement"; and Jagodzinski [136] and Yoo *et al.* [16] present a "layer displacement" mechanism where layers "rotate" their positions via vacancy diffusion. Both of these transformation mechanisms also become energetically easier by encompassing partial dislocation motion. Although the motion of partial dislocations requires a high temperature in SiC, the nucleation of the initial dislocations can require even more activation energy. Fortunately for the sake of the transformation, most single crystals of SiC have many faults which terminate internally at partial dislocations.

The aforementioned transformations in single crystals require higher temperatures and longer times than the transformation observed in polycrystalline ABC-SiC, which is consistent with other comparisons of single crystal and polycrystalline transformations [6]. This difference has been attributed to the "fast transport" that occurs in either a vapor or liquid medium between grains [6]. In fact, reported kinetic data on the rates of transformations in polycrystalline SiC [3, 6, 137, 138] appear to correlate to activation energies for grain growth [6]. (Similar observations of the grain growth coincided with the transformation in ABC-SiC [66].) No kinetic data is reported for transformations in SiC single crystals. Since the ABC-SiC transformation appears dependent on growth, however, the kinetics of growth on single crystals is considered. Measurements of thin film growth by CVD exhibit a much lower activation energy (<1 eV [124, 139]), as compared to grain growth in bulk SiC (~5 eV [3, 6, 137, 138]). It is difficult to quantitatively compare c-axis growth rates on single crystals to polycrystalline grains that are mostly elongating in ABC-SiC. Based on microstructural evidence presented in the literature, grain growth (during the transformation) is faster in ABC-SiC than other polycrystalline SiC materials which do not contain Al as an additive. Yet grain growth perpendicular to the plate-like surfaces in ABC-SiC is significantly slower than CVD film growth at comparable temperatures, with both apparently limited by nucleation of new basal planes [124, 139]. Interestingly, CVD thin film growth rates are comparable on vicinal (3° off axis) and planar α–6H single crystals, even though the former produces a β–3C film and the latter retains the α–6H structure. Also CVD film growth rates are only 10-30% faster on C-terminated surfaces vs. Si-terminated surfaces, even though surface morphologies differ [123, 124, 139]. (Both the structure issue and the noncentrosymmetric growth issue are reconsidered as unanswered questions in ABC-SiC in section *ix.*) Suffice to say that the Al-rich grain boundary phase kinetically influences nucleation of new basal planes in ABC-SiC.

Jepps and Page [6] conclude that kinetically the transformation is dominated by grain growth; but their growth is of alpha grains, and they insist stacking fault propagation is

needed to initially nucleate each alpha grain [6, 12, 13, 91, 99, 101]. Since there are many faults in a typical beta grain, nucleation of alpha on faults would result in many faults in the final alpha grain. However, the growing alpha grains always have a much lower fault density than the initial beta grains. Jepps and Page propose the transformation is a "two-step process with partial transformation within individual small beta grains occurring prior to their absorption into large α–grains by a process of plate-growth" [6]. This mechanism is not consistent with the observation of dual-phase, plate-like grains in a surrounding beta matrix during the early stage of transformation in ABC-SiC (Figure 4a).

Since the transformation kinetics dominate the final product, the grain growth kinetics are often treated as "independent" and therefore nonessential. However, it seems unlikely that both kinetic mechanisms occur independently and yet at similar rates over the wide range of temperatures (and processing conditions) reported. If the motion of partial dislocations is easiest, then the grains should transform before they grow; but submicron alpha grains are never a product of the transformation. If grain growth is easiest, then atoms will diffuse across grain boundaries and directly attach with the thermodynamically favored alpha stacking, as in ABC-SiC. The third option would be for atoms to diffuse across the grain boundary, attach with an unfavorable beta stacking, and then require additional energy to have a dislocation later change the stacking to alpha. At first this metastable growth of beta planes seems feasible, but it is reemphasized that stacking faults are easily formed when beta grows. When grains are growing even at lower temperatures, it is reasonable for the transformation to occur via the growth. However, when grains become sufficiently large that growth kinetics are diminished, then the kinetics of dislocation motion will dominate the transformation, especially as internal dislocation sources become more probable in larger crystals. Thus different transformation mechanisms become justified at different temperatures for single crystal and polycrystalline materials.

The coupling of metastable beta grain growth followed by transformation via partial dislocation motion is the essence of the model proposed by the works of Hueur [8-11] and Shinozaki [26, 51, 52, 90, 103]. Their transformation mechanism requires "sheaths" of beta phase to be sandwiching the alpha phase as it nucleates and grows in the middle of the beta grain. The growth of this "composite" grain, where the beta sheaths lower the total interfacial energy, is justified by the "extreme anisotropies of interfacial energies, between alpha and beta SiC." To account for the energy associated with sheaths of beta within which the alpha phase is sandwiched, Heuer and Shinozaki developed an energetic model that has the grain boundary between the beta sheath and the surrounding polycrystalline beta matrix, plus the boundary between the beta sheath and alpha interior total to less energy than a grain boundary between alpha and the polycrystalline beta matrix [9]. The transformation kinetics proposed by these works, i.e. of beta sheaths growing by typical grain growth and alpha thickening by motion of partial dislocations, implies independence of the two mechanisms. For a particular constant temperature, if partial dislocations move, then alpha should quickly consume all the beta sheaths. If beta grows fast by recrystallizing "old" beta, then the transformation will never go to complete alpha. Thus their interfacial energy model was developed to justify two independent

kinetic mechanisms (beta grain growth and dislocation motion) occurring together. This splitting of a boundary is energetically akin to the splitting of a dislocation to form partials and a stacking fault; i.e. the excess energy of the intermediate beta sheath must also be added to that of the two boundaries. The ΔG_{vol} of the beta sheath may not be much more than the ΔG_{vol} of alpha, but it must be sufficiently more to provide a driving force for the transformation to alpha.

The energetic condition for coupled growth of beta sheath and interior alpha phase has been calculated as: "$\gamma^{\beta/\alpha} > \gamma^{\beta r/\alpha}$" [9], where β_r represents the recrystallized beta sheath, and γ is the grain boundary energy. (This condition needs to be modified by multiplying the right-hand side of the equation by a factor of 3, or more, in order to correctly compare the same size plate-like grains with and without sheaths, since each sheath is "often much thicker than the alpha plate it encloses" [1, 9].) Since the recrystallized beta sheath and the alpha phase have a coherent interface, it is reasonable that the β_r/α interface has a lower energy. However, this model only justifies dual phase growth, similar to that observed in ABC-SiC. It does not allow for the alpha phase to thicken until all original beta grains have been recrystallized as beta sheaths. It also assumes that the recrystallized beta phase has the same energy as the original beta grains, which is inconsistent with observations of change in stacking fault density as beta grows in ABC-SiC, and other SiC materials [112]. Since the volume of beta that recrystallizes as sheaths is more than that of the growing alpha interior [9], most of the SiC will undergo a two-step transformation; first to recrystallized beta and then to alpha. This makes the volume fraction of alpha primarily dependent on the second step, which means the measured kinetics should be dominated by the activation energy for dislocation motion and not by grain growth as observed [6]. Although a two-step transformation can be reasonable for processing at two sequential temperatures, it is inconsistent with typical recrystallization in materials. Even in SiC, "recrystallizing" beta first has been shown to hinder the subsequent transformation to alpha [112]. The beta sheaths could be considered as "stacking faults" of the alpha phase, thereby providing little driving force to justify their removal, similar to the persistent beta bottoms in ABC-SiC. Furthermore, the interfacial energy model for coupled growth of beta sheaths and alpha phase does not account for how the alpha initially formed in the middle of the grain. In essence, involving sheaths makes the beta-to-alpha transformation a three-step process: nucleation and growth of a critical thickness of alpha in the middle of a grain, followed by growth of a "composite" grain involving recrystallization of beta, followed by a thickening growth of the alpha phase. Having the first and last steps dominated by partial dislocation motion, but the middle step dominated by diffusional grain growth suggests an awkward processing scenario.

An interpretation of the present ABC-SiC microstructure of dual-phase, plate-like grains with alpha on top and beta on the bottom, might suggest "half" of a beta sheath exists. The beta at the bottom of the grain could be acting as a "sheath" as proposed [8, 9, 103] to lower the energy of the alpha interface. However, it must be quickly recognized that at the later stages of growth (Figures 5a and 7a), the bottom of the plate-like grain is abutted to many other alpha grains, not residual beta powders. A beta "sheath" should not be needed to protect the alpha plate from other alpha grains. Furthermore, observation of grains such as that of Figure 7a indicate that the beta on the bottom need not be

continuous. As discussed earlier, such beta regions are connected in the third dimension, outside of the thin TEM section. However, the intermediate regions exhibit "exposed" areas of the bottom of the alpha plate, thereby indicating it also need not be sheathed.

The works of Heuer and Shinozaki show alpha plate-like grains readily elongate to consume surrounding beta matrix grains, which means all non-basal facets of the alpha phase are directly exposed to the original beta grains. Their interpretation is that only the basal facet of the alpha phase has a high energy when exposed to randomly-oriented, original beta grains; and only for the case of a coherent interface does the α basal facet produce a low energy grain boundary. Granted this coherent interface has a low energy (i.e. that of a stacking fault), but it is unclear why the basal facet of the alpha phase should have a much higher energy as a grain boundary with polycrystalline beta grains than all the other alpha facets. In fact this basal facet of the alpha phase is identical to a {111} beta facet; and the formation of plate-like morphologies indicate this is the lowest energy of all alpha facets.

In partially transformed ABC-SiC, it is this interface between the top α basal facet and the original polycrystalline beta grains that is most common (Figure 4a), and therefore energetically favorable. Furthermore, high resolution imaging determines the presence of an amorphous phase along the grain boundary (Figure 5b), with the same thickness of ~1 nm observed for β/β boundaries, β/α boundaries, and α/α boundaries [66, 69, 73]. This means a SiC grain boundary is actually two interfaces with a glassy phase sandwiched between them; and calculations [140, 141] indicate the two interfaces are energetically favorable to a singular grain boundary in nonoxide ceramics. With impurities typically enriched at grain boundaries in SiC, it seems unlikely that the energy of a boundary is much affected by whether the original polycrystalline beta matrix meets a (111) facet of recrystallized beta or a (000z) facet of an alpha polytype (i.e. $\gamma^{\alpha/\beta} \approx \gamma^{\beta r/\beta}$). If there is enough thermodynamic driving force to justify forming the alpha phase, it is going to form where it is easiest, i.e. as a stacking on a basal facet as the grain grows. Putting a beta sheath in the way appears to be complex and unnecessary.

If sheaths of recrystallized beta are not energetically necessary to "protect" the nucleating alpha phase, then why do the works of Heuer and Shinozaki observe them? Once a composite grain with sheaths has been formed, it may be expected to continue elongated growth as a composite grain. This is basically the same as elongated growth of dual-phase grains presented in ABC-SiC. When the alpha phase grows in a plate-like fashion, it can pull planes of beta along with it, as if they were stacking faults within the alpha phase. The parallel faults in beta and alpha regions of the grains actually encourage the elongated growth.

The problem arises as to how the composite grain is initially formed. Two solutions appear to both exist in their microstructures, possibly due to different processing conditions. In some cases the beta "sheaths" appear to have formed during a cored-growth process; yet in other cases no sheaths may exist. For cored growth, the beta phase would have to grow on the alpha phase. Other studies have observed the growth of beta

phase on the alpha phase, both as an epitaxial film on an α single crystal [122, 123, 124, 139] and as an outer layer of a cored polycrystalline alpha microstructure [90]. When beta is epitaxially grown on an alpha single crystal, DPB's are observed [122], which indicates multiple nucleation events and results in nonplanar growth. Additives and processing environments (especially lower temperatures) which enhance nucleation may encourage beta formation as $\{\bar{1}11\}$-type facets can develop. The sheaths in Heuer and Shinozaki micrographs [8, 103] exhibit irregular boundaries suggestive of $\{\bar{1}11\}$ faceting. The "as received" microstructure of the Heuer works [8] exhibits elongated shapes suggesting alpha plates already exist as "seeds", onto which the recrystallized beta appears to grow at a low temperature. At higher temperatures, the alpha seeds elongate to consume much of the original beta. Thus the appearance of beta sheaths in metallographic images may be representative of a cored growth with processing conditions (including additives) that stabilize beta growth on alpha basal surfaces, rather than necessary for a transformation mechanism [8, 10, 11, 52, 90, 103].

Secondly, bright field TEM images presented in the works of Heuer and Shinozaki [8, 51, 52, 103], as well as other TEM investigations, appear quite similar to the images presented here and elsewhere [68, 69, 72] for ABC-SiC. Reported electron diffraction exhibits strong evidence of α–4H in the α–6H grains [51, 52]; features similar to the beta-seed portion of ABC-SiC grains appear in images of plate-like alpha grains [51, 103]; and Shinozaki has recently observed that some alpha grains lack beta sheaths [51]. On the other hand, bright field TEM images have been produced through tilting experiments on this ABC-SiC [72] which suggest a similarity to the "sheaths" observed in the Heuer and Shinozaki works. When a grain is tilted more than a couple degrees from the $[\bar{2}110]$ zone axis, the contrast within a grain becomes dominated by the tilted stacking faults. A stripe of different contrast through the middle of a plate-like grain can represent a variation in stacking fault density [72], rather than a different phase sandwiched in the middle of the grain [8, 90]. Although twins commonly result in bright field contrast in the beta phase, these reflection twins do not exist in the 4H and 6H structures. Dark field imaging has been used to differentiate the different twins in a beta grain [90]; however, "clean" two-beam dark field images are difficult to acquire to resolve polytypes in SiC because of the close proximity of the reflections.

When a grain is imaged exactly on the $[\bar{2}110]$ zone axis, no contrast difference exists between regions of different phases nor from twins and faults. Tilting only a few milliradians from the zone axis, however, can have dramatic effects on the phase contrast. Typically this effect is noticed in ("all" [102]) high resolution lattice images, but some phase contrast also exists in most bright field images of alpha polytypes because the image incorporates part of the [0001] diffracted beam as well as the transmitted beam. Thus minimal tilts can alter the relative contrast of two α–4H regions within a grain that are separated by a stacking fault [72], and give rise to BF images that are suggestive of beta sheaths. Yet HR-TEM and electron diffraction never detect a beta sheath during growth up from the top alpha facet in ABC-SiC. [It is noted that the TEMs utilized at the time of the earlier works had insufficient resolution to provide cross-lattice fringes to unambiguously determine the polytype of each plane. Similarly, selected area diffraction can analyze smaller regions of grains in modern (Topcon 002B) microscopes.]

As different processing methods have reported different transformation mechanisms and products, so have there also been observed different grain morphologies. Single crystals have been grown in equiaxed, needle (whisker), and plate shapes [3, 129, 142]. When crystals of various polytypes are simultaneously produced, those comprised of mixed polytypes are often plate-like, whereas equiaxed crystals typically exhibit only one polytype [82, 129]. Transformations of α–2H whiskers to the beta phase by vapor transport resulted in more-equiaxed crystals [3]. However, transformations in large single crystals often do not involve shape changes [86]. Both alpha and beta phases of polycrystalline SiC have been observed as equiaxed or plate-like grains, but the presence of polycrystalline needles is rarely observed [49]. No TEM analyses have been reported for "plate-like beta grains" [61, 62], other than the minor elongations observed in this study (Figure 3a), as a consequence of parallel faults. Grains comprised of two phases may also be either plate-like when the two phases grow concurrently (for example in the dual-phase grains of ABC-SiC and in the "composite" grains of the Heuer works [8-11]), or equiaxed if they undergo cored growth [90, 92]. α–4H grains are often observed as being plate-like [45-52], such as in ABC-SiC. The morphology of alpha grains may be dependent on internal stacking faults as well as crystal structure. α–6H grains that are plate-like often have (parallel) internal faults [8-11, 103], whereas equiaxed α–6H grains such as those in Hexoloy SA are fault-free [73].

In addition to being the theoretical equilibrium high-temperature phase, the α–6H structure also has symmetrical arrangements similar to that of the cubic structure which may be expected to affect the morphology of the hexagonal grains. For example the $\{\bar{1}102\}_{6H}$ planes have regions of close packing and a d-spacing the same as that of the basal {000z} planes. Thus such surfaces may be expected to form similar low energy facets, enabling the α–6H structure to form equiaxed grains. Such equiaxed grains have been exhibited in numerous SiC materials having the α–6H structure, the most common being the commercial material, Hexoloy SA [64, 65, 73]. However, if/when 6H grains have a high density of stacking defects, doubtlessly parallel to the basal plane, such 6H grains may be expected to develop an elongated nature as they grow. A recent report [63] discusses two SiC ceramics, one being processed from only equiaxed 6H powders, and the second processed from a mixture of the equiaxed 6H powders and a second 6H powder. No assessment of defect structures within the powders was presented. Whereas the pure equiaxed powders retained their shape as they slowly grew, the second 6H powders grew with an elongated nature and "took-over" the overall microstructure. (This same second group of powders have also been observed by another group as producing an elongated microstructure [56].) The α–4H structure does not have planes other than (0001) that can develop low energy facets; thus even relatively fault-free, α–4H grains continue plate-like growth (Figure 7a). Therefore the morphology of the developing microstructure is not only dependent on the polytype which forms, but also upon defect structure within the grains. In addition, the sintering additives used not only affect the temperature of transformation and the structure of the transformation product, but also the internal defect structure which influences the microstructure morphology. Such internal defect structure can only be unambiguously studied by transmission electron microscopy.

The growth-induced transformation could account for different phases, different morphologies, and different XRD analyses depending on the temperature(s) at which SiC has been processed. If the transformation occurs at a "low" temperature, a large mixed-phase region will be formed and many faults can be grown into the top α–4H region. The faults plus the 4H structure will lead to an elongated morphology with a high aspect ratio; however, overall growth will be slow due to the low temperature. The presence of many faults will produce XRD results that erroneously suggest mostly beta is present. If the transformation occurs at a medium temperature, large regions of low-fault α–4H will produce an elongated morphology, and XRD will correctly assess the 4H structure. If the transformation occurs at a higher temperature (>1900°C), α–6H may begin to form due to its thermodynamic preference. This can lead to grains having mixed α–4H and α–6H, and consequently the many faults will enhance elongated growth morphologies, but will disrupt the XRD analysis such that it suggests beta exists. If the transformation occurs at a very high temperature, only α–6H will form; with faults being less prominent, grain growth being equiaxed, and XRD analyses assessing the correct alpha phase. Unfortunately, it is difficult to apply high temperature processing without experiencing some initial lower-temperature processing. Thus in practice a two-stage transformation is quite possible. One example could start with the development of elongated α–4H grains at a lower temperature. Later at a higher temperature the α–6H will want to form. If the grains have already grown sufficiently large that the driving force for continued growth has diminished, and if/when the temperature becomes sufficient to activate partial dislocation motion, the α–4H to α–6H transformation can occur by dislocation motion. Since the region of the α–4H grain that formed at the lowest temperatures has more faults, and the mixed phase region has many faults, the highest density of faults will typically be near the middle of the grain. Thus α–6H will nucleate on these many stacking faults in the middle of the grain, thereby developing a composite grain. (Other metastable and/or stable alpha polytypes, such as 15R, would also be expected to form in a similar location.)

When all SiC materials are exposed to very high temperature processing (>2400°C), eventually all will transform to an equiaxed α–6H microstructure with minimal faults. Thus the introduction of α–6H seeds can influence morphologies at lower temperatures, and additives can alter the temperature ranges at which kinetic mechanisms are active and particular phases are thermodynamically stable.

ix) A Couple Unanswered Questions (?)

The growth-induced transformation observed in ABC-SiC has produced a number of unanswered questions, a couple of which are considered here, with the intention that future work may provide some answers. These ABC-SiC grains grow "up" from a beta seed and continue growing "up" as the alpha phase. Why don't the beta grains grow down in the$[000\bar{1}]_H$ direction? In fact, if they grew in both directions, a cored-growth process would develop elongated composite grains with the beta phase in the middle and alpha "sheaths" on the outside, having a structural arrangement just opposite to that reported in the Heuer and Shinozaki works. Three reasons are considered to affect this asymmetric growth rate.

First, the "bowl-like" shapes of the beta grains are such that the bottom surface never exhibits as large a smooth facet as the top. This may prevent the development of a sufficiently large critical nucleus of the α–4H phase. However, this "bowl-like" shape of a beta grain is believed to be a consequence and not a cause of [111] growth being faster than $[\bar{1}\bar{1}\bar{1}]$ growth. Secondly, the dramatic increase in elongated growth rate of these dual-phase grains causes them to impinge upon each other at an early stage in the transformation process. This means the top hexagonal surface will have another plate-like grain impinging it. But this hexagonal surface can continue to slowly grow, as it will be consuming higher energy facets of the impinging grain(s). The bottom beta surface would also have dual-phase plates impinging it. Nucleation and growth of new alpha planes on this beta surface would be difficult, as there are already alpha grains present that would have to be consumed. During later stages of the transformation it becomes even more difficult for alpha planes to form on this bottom beta surface. Again, this impingement problem is believed to be a consequence rather than a cause of the one-directional growth.

A third reason considers that the [111] (or [0001]) and $[\bar{1}\bar{1}\bar{1}]$ (or $[000\bar{1}]$) directions and their corresponding planes are not equivalent because the zincblende (and wurtzite) structures are not centrosymmetric. One basal facet is terminated with a Si-[0001] surface, while the opposite side is terminated by a C-$[000\bar{1}]$ surface. Growth rates (as well as etch rates) are commonly different for the two directions in compound semiconductors, although growth of heteroepitaxial films of α-6H by CVD are measured as only 10% - 30% faster on the C-surfaces than on the Si-surfaces [115, 123, 124, 139]. Enhanced nucleation on the C-surfaces of single crystals speed their growth but also results in a rougher surface morphology [123, 124]. This is in contrast to the plate-like ABC-SiC grains which grow faster perpendicular to the smooth top surface than the rough bottom surface. With growth being limited by nucleation, it is more appropriate to think of the Si-surface growth as slower on single crystals (rather than C-surface growth as faster). Surface reconstruction of the Si-surface above 1100°C results in the formation of a graphite-like layer as Si vaporizes, and this is expected to hinder nucleation of the next layer [114, 115, 124]. Since nucleation of a new basal layer is even more difficult during grain growth in ABC-SiC (on both C-surfaces and Si-surfaces), complex surface reconstructions involving Al and O may exist and hamper nucleation, even if they do not exhibit long range order across an entire grain boundary facet.

Platelets (~1 mm long and ~0.01 mm thick) of another wurtzite structure, GaN, have recently been produced with atomically flat tops and rough, faceted bottoms, with the different surface morphology attributed to the different chemistry (and/or surface reconstructions) on each side of the crystal [125]. Although the rough morphology of the bottom of the platelets would appear to ease interface attachment growth, the flat tops of these GaN platelets are believed to grow faster [125], similar to the plate-like ABC-SiC grains. Asymmetric growth rates resulting from the noncentrosymmetric structure are more probable for a TLK nucleation involving pillboxes, since growth of polytypes about screw dislocations would provide sites for both C and Si attachment on both sides of the grain. On the other hand, screw dislocations could account for the similar growth rates sometimes reported for both sides of single crystals [80]. The difference between the growth rates for the two directions is not easily calculated in ABC-SiC because of the presence of the grain boundary phase comprised of sintering additives and oxygen from the native oxide on the powders. However, the additives and/or different temperature regimes are expected to alter the relative growth rates of the two sides. Physical surface reconstructions of grain facets in a liquid medium are difficult to propose; however, chemical effects can be considered. The graphite-like reconstruction that exists on the Si-surfaces of single crystals is not believed to be present on ABC-SiC grains, because of both the excess O present in grain boundary layers and the inability of Si to "vaporize" inside a bulk SiC material. Since excess Si and C atoms will be diffusing through the grain boundary phase, sources of ad-atoms do not appear to be rate-limiting. Rather the removal of adsorbed impurities may influence the growth rates. Aluminum and other metallic atoms may temporarily adsorb, but they should be readily redissolved and replaced by absorbed Si atoms. However, on the Si-terminated facet, oxygen will get adsorbed (or even persist from the original native oxide on the powder) and be difficult to replace with the C necessary for growth. Since sintering SiC is much "easier" at temperatures above 2000°C, such asymmetric growth rates may not be evident at all temperatures. Optical micrographs of cored growth in other SiC materials suggest growth can occur in both directions [8, 91, 103]. However, in the temperature range where removal of oxygen from the SiC surface is difficult, grains may be expected to grow faster in the C-terminated direction. The present analysis has not resolved whether all α–4H grains grow "up" from the C-surfaces. In HR-TEM image simulations subtle tilts and changes in defocus can correspond to ambiguities in orientation [102]. Attempts to use ALCHEMI [143] and Convergent Beam Electron Diffraction [125, 144] to determine the crystal polarity have thus far been unsuccessful due to the distortions caused by the close spacing of faults within each grain.

Based on the observations in ABC-SiC, grain growth is a necessary requirement in order to invoke the phase transformation (at temperatures between 1700°C and 1900°C). A second question arises: if grain growth is experimentally inhibited, will the transformation be prevented? The same ABC-SiC alloys have been processed with added yttria particles [70], with less grain growth and less transformation observed. If fine, undissolved, yttria particles inhibit grain boundary motion, then growth will be sluggish during densification. When these yttria-containing materials are processed at temperatures above 1900°C, the transformation begins to slowly occur, and the

transformation product is primarily α–6H. Other reports have utilized a mixture of alumina and yttria (>10 vol. %) and obtained substantial elongated grain growth [45-48]; however, these materials are expected to have only an amorphous phase at the grain boundaries, similar to silicon nitride materials with similar additives [76, 78, 141]. The addition of Mg as an alloy to the aluminum in these ABC-SiC materials has also appeared to slow both the growth and the transformation rates, due to the formation of a more-stable, spinel, secondary phase [109]. When grain growth is inhibited and growth-induced transformation prevented, a dislocation-induced transformation may be invoked at higher temperatures. In the single crystal model of Pirouz [7] partial dislocations must cross-slip and the thermal activation energy to nucleate these dislocations may be more than for grain boundary diffusion through a liquid phase. If/when sintering and grain growth are controlled by bulk diffusion through the SiC grains, then climb and cross-slip of dislocations will be more probable, and the dislocation-induced transformation can be activated.

Other research efforts have noted additives that enhance sintering but prevent the transformation, and typically these final SiC microstructures exhibit a smaller grain size [6, 29, 30, 37, 38, 145]. Beta SiC has been processed with oxide additives to prevent the transformation because the transformation often prevented full densification. The intention was to produce a dense, equiaxed, fine-grain beta microstructure with optimum mechanical properties. Traditionally, finer grain size has meant smaller flaws and higher toughness in SiC [146]. In the present ABC-SiC research, the transformation with elongated grain growth (in an already dense medium) provides interlocking that causes the strength to be improved as the grains grow longer. Further improvement in properties are directed toward enhancing the transformation in order to increase aspect ratio and further increase the interlocking. Thus grain growth and transformation have become more desirable, and the question of inhibiting both is yet to be studied.

A third unresolved issue arises from both of the above unanswered growth questions; that is, what are the equilibrium phases of SiC at different temperatures? Most experimentalists and theoreticians agree that at the highest temperatures (especially >2400°C) SiC will exhibit the α–6H structure, independent of what impurities are present. However, the slow kinetics of the reverse transformation(s) make the relative stability of low temperature phase(s) less clear. The α–4H structure has been calculated as the equilibrium phase at all temperatures below ~2000°C, based on either *ab initio*, phonon-free-energy calculations [17, 84, 85] or stacking fault energies [18]. Experimentally, the formation of α–4H may result from only the inclusion of Al [23-26, 28, 39, 49, 51, 52, 80] or another impurity. However, Al is the most prominent unintentional impurity in semiconductor-grade single crystals of both α–6H and α–4H [123, 124, 147]. The presence of higher unintentional dopant levels ($>10^{19}$ / cm^3) in α–4H single crystals may again be the result of kinetic (processing) issues rather than the α–4H phase stability's dependence on Al. With SiC growth's strong limitation by the nucleation of each basal layer, a kinetic (or catalytic) role played by the Al seems more probable than a thermodynamic necessity for α–4H formation. Once a β–3C, α–4H, α–6H or any stacking fault layer is nucleated, it grows to the radial extremes of the grain, and this strong desire to propagate faults during growth seems to preclude a dependence

of phase stability on impurity concentration. Only in solid solutions, such as the α–2H SiC / AlN [32, 148], do other elements play a clear role in controlling the phase stability of SiC.

Based on theory, β–3C only nucleates as a metastable phase due to kinetic limitations; for example, small crystals with a cubic structure and multiple {111} facets have relatively lower surface energy than a small alpha crystal. However, some experimental evidence indicates β–3C is the equilibrium phase below some nominal (possibly ~1600°C) temperature. For example, ABC-SiC hot pressed at 1600°C - 1650°C only exhibits the β–3C structure, even though grains have grown during densification [44, 66, 94]. The final one micron grain size would seem to be of sufficient size to justify nucleating the hexagonal structure, if it is thermodynamically desirable at 1600°C. Even when >5% Al is added, no α–4H formation is observed during grain growth at temperatures below 1700°C [44, 66, 94]. The reduction in stacking fault density for the β–3C phase grown above 1700°C also supports the thermodynamic stability of the β–3C phase. Since ABC-SiC grains never grow around crystalline triple points (Figure 7c), grain growth is essentially stopped below ~1600°C, making it kinetically impossible to establish what phase is thermodynamically stable at lower temperatures in ABC-SiC.

The CVD growth of β–3C thin films on planar α–6H single crystals in the temperature range of 1400°C to 1700°C [123, 124] initially seems to establish the thermodynamic stability of the β–3C phase. However, such films typically develop a rough morphology as a result of initial nucleation occurring as pyramidal-shape islands [124]. These islands are truncated on top by the three low-energy $\{\bar{1}11\}$ facets of the cubic structure, even after growing to >2 microns in width. Thus it becomes conceivable that the low energy nature of {111} facets justifies the nucleation, and even the growth to >1 micron, of powders, grains, and thin films of β–3C as a metastable phase.

It may seem difficult to fully understand and control the beta-to-alpha transformation in SiC, when the thermodynamic stability of phases is not well established. Yet in ABC-SiC, the transformation is kinetically controlled by grain growth, which in turn is judiciously controlled to provide a high-toughness, high-strength material.

CONCLUSIONS

SiC processed with Al, B, and C undergoes a transformation from the cubic to the hexagonal phase, which is documented by interactive HR-TEM, XRD, and SEM analyses. The transformation occurs as grains grow and the stacking converts from β–3C to α–4H. Elongated growth develops plate-like, dual-phase grains with an atomically flat top terminating the alpha phase and a multi-faceted bottom terminating the beta phase. The beta-to-alpha transformation has historically been a bane to mechanical properties, because when the transformation to a plate-like morphology occurs prior to densification it can inhibit densification. In these hot pressed ABC-SiC materials the transformation is controlled to occur after full densification. Processing above 1850°C produces a completely interlocking, plate-like microstructure with record toughness [75] and high strength [66]; yet the initial beta seed portions of grains are retained. A thin (~1 nm) amorphous phase at the grain boundaries enhances sintering and interface attachment kinetics; however, the macroscopic driving force is akin to Ostwald ripening. Partial dislocation motion is not instrumental in this growth-induced transformation.

ACKNOWLEDGMENTS

The authors wish to acknowledge the students, M. Gopal, M. Chandramouli, C. Gilbert, M. Sixta, and Y. He, in the research groups of Professors G. Thomas, R. Ritchie, and L. De Jonghe for critiques of this manuscript and helpful discussions. The staff members of the National Center for Electron Microscopy at LBL are thanked for the utilization of microscopes and accessory equipment. This work was funded by the U. S. Dept. of Energy, Office of Basic Energy Sciences, Materials Science Division under Contract # DE-AC03-76SF00098.

REFERENCES

1. W. F. Knippenberg, "Growth Phenomena in Silicon Carbide," *Philips Res. Rept.*, **18**, 161-274 (1963).

2. A. R. Verma and P. Krishna, in Polymorphism and Polytypism in Crystals, J. Wiley & Sons, 113 (1966).

3. G. A. Bootsma, W. F. Knippenberg, and G. Verspui, "Phase Transformations, Habit Changes and Crystal Growth in SiC," *J. Crystal Growth*, **8**, 341-353 (1971).

4. P. Krishna and R. C. Marshall, "The Structure, Perfection and Annealing Behaviour of SiC Needles Grown by a VLS Mechanism," *J. Crystal Growth*, **9**, 319-325 (1971).

5. D. Pandey and P. Krishna, "Mechanism of Solid State Transformations in Silicon Carbide, in Silicon Carbide, ed. R. C. Marshall, J. W. Faust, and C. E. Ryan, U. South Carolina Press, 198-206 (1973).

6. N. W. Jepps and T. F. Page "Polytypic Transformations in Silicon Carbide," in Prog. Crystal Growth and Characterization, ed. P. Krishna, Pergamon Press, **V7**, 259-307 (1983).

7. P. Pirouz and J. W. Yang, "Polytypic Transformations in SiC: the Role of TEM," *Ultramicroscopy*, **51**, 189-214 (1993).

8. A. H. Heuer, G. A. Fryburg, L. U. Ogbuji, and T. E. Mitchell, "The β to α Transformation in Polycrystalline SiC: I, Microstructural Aspects," *J. Am. Ceram. Soc.*, **61** [9] 406-412 (1978).

9. T. E. Mitchell, L. U. Ogbuji, and A. H. Heuer, "The β to α Transformation in Polycrystalline SiC: II, Interfacial Energies," *J. Am. Ceram. Soc.*, **61** [9] 412-413 (1978).

10. L. U. Ogbuji, T. E. Mitchell, and A. H. Heuer, "The β to α Transformation in Polycrystalline SiC: III, The Thickening of a Plates," *J. Am. Ceram. Soc.*, **64** [2] 91-99 (1981).

11. L. U. Ogbuji, T. E. Mitchell, A. H. Heuer, and S. Shinozaki, "The β to α Transformation in Polycrystalline SiC: IV, A Comparison of Conventionally Sintered, Hot-Pressed, Reaction-Sintered, and Chemically Vapor-Deposited Samples," *J. Am. Ceram. Soc.*, **64** [2] 91-99 (1981).

12. N. W. Jepps and T. F. Page, "Electron Microscopy of Interfaces Between Transforming Polytypes in Silicon Carbide," *J. Microscopy,* **116** [1] 159-171 (1979).

13. N. W. Jepps and T. F. Page, "Intermediate Transformation Structures in Silicon Carbide," *J. Microscopy*, **119** [1] 177-188 (1980).

14. P Pandey and P. Krishna, "The Origin of Polytype Structures," in Prog. Crystal Growth and Characterization, ed. P. Krishna, Pergamon Press, **V7**, 213-258 (1983).

15. M. T. Sebastian and P. Krishna, "Single Crystal Diffraction Studies of Stacking Faults in Close-Packed Structures," in Prog. Crystal Growth and Characterization, Pergamon Press, **V14**, 103-183 (1987).

16. W. S. Yoo and H. Matsunami, "Solid-State Phase Transformation in Cubic Silicon Carbide," *Jap. J. Appl. Phys.*, **30** [3] 545-553 (1991).

17. C. Cheng, V. Heine, and I. L. Jones, "Silicon Carbide Polytypes as Equilibrium Structures," J. *Phys. Condensed Matter*, , **2** 5097-5113 (1990).

18. F. R. Chien, S. R. Nutt, and W. S. Yoo, "Stacking Fault Energy Calculations in 6H- and 15R-SiC," MRS Proceedings, Spring (1994).

19. D. Lundquist, "On the Crystal Structure of Silicon Carbide and Its Content of Impurities," *Acta Chem. Scand.*, **2**, 171 (1968).

20. E. D. Whitney and P. T. B. Shaffer, "Investigation of the Phase Transformation Between α– and β–Silicon Carbide at High Pressure," *High Temperatures - High Pressures*, **1**, 107-110 (1969).

21. Y. Inomata, Z. Inoue, and K. Kijima, "On the Formation of the 15R Type in the β–α Transformation of SiC," *Yogyo-Kyokai-Shi*, **77**, [9] 313-318 (1969).

22. P. Krishna, R. C. Marshall, and C. E. Ryan, "The Discovery of a 2H-3C Solid State Transformation in Silicon Carbide Single Crystals," *J. Crystal Growth* **8**, 129-131 (1971).

23. R. M. Williams, B. N. Juterbock, S. Shinozaki, C. R. Peters, and T. J. Whalen, "Effects of Sintering Temperatures on the Physical and Crystallographic Properties of β–SiC," *Amer. Ceramic Soc. Bulletin*, **64** [10] 1385-1389 (1985).

24. S. Shinozaki, R. M. Williams, B. N. Juterbock, W. T. Donlon, J. Hangas, and C. R. Peters, "Microstructural Developments in Pressureless-Sintered β–SiC Materials with Al, B, and C Additions," *Amer. Ceramic Soc. Bulletin*, **64** [10] 1389-1393 (1985).

25. D. H. Stutz, S. Prochazka, and J. Lorenz, "Sintering and Microstructure Formation of β–Silicon Carbide," J. *Am. Ceram. Soc.*, **68** [9] 479-482 (1985).

26. S. Shinozaki, J. Hangas, K. Maeda, A. Soeta, "Enhanced Formation of 4H Polytype in Silicon Carbide Materials," in Silicon Carbide Ceramics 87, *Amer. Ceramic Soc. Transactions*, 113-121 (1987).

27. M. Srinivasan, "The Silicon Carbide Family of Structural Ceramics," Treatise on Materials Science and Technology, Academic Press, **V29**, 99-159, (1987).

28. K. Suzuki, "Pressureless-Sintered Silicon Carbide with Addition of Aluminum Oxide," in Silicon Carbide Ceramics V2, ed. S. Somiya and Y. Inomata, Elsevier Applied Science, 163-182 (1991).

29. M. Omori and H. Takei, "Preparation of Pressureless-Sintered SiC-Y_2O_3-Al_2O_3," *J. Matls. Sci.*, **23**, 3744-3749 (1988).

30. E. Kostic, "Sintering of Silicon Carbide in the Presence of Oxide Additives," *Powder Metallurgy International*, **20** [6] 88-89 (1988).

31. M. A. Mulla and V. D. Krstic, "Low-Temperature Pressureless Sintering of β–Silicon Carbide with Aluminum Oxide and Yttrium Oxide Additions," *Ceram. Bull.*, **70** [3] 439-443 (1991).

32. Y. Xu, A. Zangvil, M. Landon, and F. Thevenot, "Microstructure and Mechanical Properties of Hot-Pressed Silicon Carbide - Aluminum Nitride Compositions," *J. Amer. Ceramic Soc.*, **75** [2] 325-333 (1992).

33. N. W. Jepps and T. F. Page, "The 6H - 3C 'Reverse' Transformation in Silicon Carbide Compacts," *J. Amer. Ceramic Soc.*, **64** [12] C177-C178 (1981).

34. J. W. Yang and P. Pirouz, "The α–β Polytypic Transformation in High-Temperature Indented SiC," *J. Mater. Res.*, **8** [11] 2902-2907 (1993).

35. R. S. Ramsdell, "Studies in Silicon Carbide," *Amer. Min.*, **32**, 64-82 (1947).

36. R. A. Alliegro, L. B. Coffin, and J. R. Tinklepaugh, "Pressure-Sintered Silicon Carbide," *J. Amer. Ceramic Soc.*, **39** [11] 386-389 (1956).

37. F. F. Lange, "Hot-Pressing Behaviour of Silicon Carbide Powders with Additions of Aluminum Oxide," *J. Matls. Sci.*, **10**, 314-320 (1975).

38. S. Prochazka and R. M. Scanlan, "Effect of Boron and Carbon on Sintering of SiC," *J. Amer. Ceramic Soc.*, **58** [1] 72 (1975).

39. Y. Tajima and W. D. Kingery, "Solid Solubility of Aluminum and Boron in Silicon Carbide," *J. Amer. Ceramic Soc.*, **65** [2] C27-C29 (1982).

40. R. Hamminger, G. Grathwohl, and F. Thummler, "Microanalytical Investigation of Sintered SiC, Part I: Bulk Material and Inclusions," *J. Matls. Sci.*, **18**, 353-364 (1983).

41. K. Negita, "Effective Sintering Aids for Silicon Carbide Ceramics: Reactivities of Silicon Carbide with Various Additives," *J. Amer. Ceramic Soc.*, **69** [12] C308-C310 (1986).

42. K. Nakamura and K. Maeda, "Hot-pressed SiC Ceramics," in Silicon Carbide Ceramics V2, ed. S. Somiya and Y. Inomata, Elsevier Applied Science, 139-162 (1991).

43. H. Tanaka, "Sintering of Silicon Carbide," in Silicon Carbide Ceramics V1, ed. S. Somiya and Y. Inomata, Elsevier Applied Science, 213-238 (1991).

44. T. D. Mitchell, L. C. DeJonghe, W. J. MoberlyChan, & R. O. Ritchie, "Silicon Carbide Platelet / Silicon Carbide Composites", *J. Am. Ceram. Soc.*, **78** [1], 97-103 (1995).

45. D. H. Kim and C. H. Kim, "Toughening Behavior of Silicon Carbide with Additions of Yttria and Alumina," *J. Am. Ceram. Soc.*, **73** [5] 1431-1434 (1990).

46. S. K. Lee and C. H. Kim, "Effects of α–SiC versus β–SiC Starting Powders on Microstructure and Fracture Toughness of SiC Sintered with Al2O3 - Y2O3 Additives," *J. Amer. Ceramic Soc.*, **77** [6] 1655-1658 (1994).

47. N. P. Padture, "*In Situ*-Toughened Silicon Carbide," *J. Amer. Ceramic Soc.*, **77** [2] 519-523 (1994).

48. N. P. Padture and B. R. Lawn, "Toughness Properties of a Silicon Carbide with an *in situ* Induced Heterogeneous Grain Structure," *J. Amer. Ceramic Soc.*, **77** [10] 2518-2522 (1994).

49. M. A. Mulla and V. D. Krstic, "Mechanical Properties of β–SiC Pressureless Sintered with Al_2O_3 Additions," *Acta Metall. Mater.*, **42** [1] 303-308 (1994).

50. M. A. Mulla and V. D. Krstic, "Pressureless Sintering of β–SiC with Al_2O_3 Additions," *J. Matls. Sci.*, **29**, 934-938 (1994).

51. S. S. Shinozaki, J. Hangas, K. R. Carduner, M. J. Rokosz, K. Suzuki, and N. Shinohara, "Correlation Between Microstructure and Mechanical Properties in Silicon Carbide with Alumina Addition," *J. Mater. Res.*, **8** [7] 1635-1643 (1993).

52. S. S. Shinozaki, "Unique Microstructural Development in SiC Materials with High Fracture Toughness," *Matls. Res. Soc. Bull.*, Feb. 42-45 (1995).

53. V. D. Krstic, "Optimization of Mechanical Properties in SiC by Control of the Microstructure," *Matls. Res. Soc. Bull.*, Feb. 46-48 (1995).

54. E. J. Winn and W. J. Clegg, "The Processing of In-Situ Toughened Ceramics," oral presentation at Amer. Ceramic Soc., New Orleans Nov., (1995).

55. M. J. Hoffman, "In-Situ Toughening of Non Oxide Ceramics," oral presentation at Amer. Ceramic Soc., New Orleans Nov., (1995).

56. S. H. Robinson, D. J. Shanefield, and D. E. Niesz, "Microstructural Control of Silicon Carbide Via Liquid Phase Sintering," oral presentation at Amer. Ceramic Soc., New Orleans Nov., (1995).

57. B. E. Warren, in X-Ray Diffraction, Dover Publ., 251-314 (1990).

58. S. Shinozaki and K. R. Kinsman, "Aspects of 'One Dimensional Disorder' in Silicon Carbide," *Acta Metall.*, **26**, 769-776 (1978).

59. M. Farkas-Jahnke, "Structure Determination of Polytypes," in Prog. Crystal Growth and Characterization, ed. P. Krishna, Pergamon Press, **V7**, 163-211 (1983).

60. S. G. Cook, J. A. Little, and J. E. King, "Etching and Microstructure of Engineering Ceramics," *Matls. Charact.*, **34** [1] 1-8 (1995).

61. Y. W. Kim, M. Mitomo, and H. Hirotsuru, "Grain Growth and Fracture Toughness of Fine-Grained Silicon Carbide Ceramics," *J. Amer. Ceramic Soc.*, **78** [11] 3145-3148 (1995).

62. T. Ohji and L. C. De Jonghe, "Presintering Heat Treatment, Densification, and Mechanical Properties of Silicon Carbide," *J. Amer. Ceramic Soc.*, **77** [6] 1685-1687 (1994).

63. Y. W. Kim, K. S. Cho, and J. G. Lee, "Effect of Large α–Silicon Carbide Seed grains on Microstructure and Fracture Toughness of Pressureless Sintered α–Silicon Carbide, *J. Amer. Ceramic Soc.*, submitted (1995).

64. S. Dutta, "Sinterability, Strength and Oxidation of Alpha Silicon Carbide Powders," *J. Matls. Sci.*, **19,** 1307-1313 (1984).

65. K. Y. Chia and S. K. Lau, "High Toughness Silicon Carbide," *Ceram. Eng. Sci. Proc.* **12** [9-10] 1845-1861 (1991).

66. J. J. Cao, W. J. MoberlyChan, L. C. De Jonghe, C. J. Gilbert, and R. O. Ritchie, "*In Situ* Toughened Silicon carbide with Al-B-C Additions," *J. Amer. Ceramic Soc.*, **79** [2] 461-469 (1996).

67. W. J. MoberlyChan, J. J. Cao, M. Y. Niu, and L. C. De Jonghe , "SiC Composites with Alumina-Coated α-SiC Platelets in β-SiC Matrix", Microbeam Analysis (EMSA 1994), edited by J. Friel, VCH Publishers, NY, 49-50 (1994).

68. W. J. MoberlyChan, J. J. Cao, M. Y. Niu, and L. C. De Jonghe , "Toughened β-SiC Composites with Alumina-Coated α-SiC Platelets", in High Performance Composites, edited by K. K. Chawla, TMS, 219-229 (1994).

69. W. J. MoberlyChan, J. J. Cao, and L. C. De Jonghe, "Formation of an Interlocking Microstructure with High Strength and High Toughness in Silicon Carbide Ceramics," oral presentation at Amer. Ceramic Soc., New Orleans, Nov., (1995).

70. M. E. Sixta, W. J. MoberlyChan, J. J. Cao, and L. C. De Jonghe, "Processing and Characterization of Yttria-Coated SiC-Platelet / SiC Composites," presentation at Amer. Ceramic Soc., Cincinnati, May, (1995).

71. J. J. Cao, W. J. MoberlyChan, L. C. De Jonghe, B. Dalgleish, and M. Y. Niu, "Processing and Characterization of SiC Platelet / SiC Composites," in Advances in Ceramic-matrix Composites II, Ceramic Transactions, **46**, 277-288 (1994).

72. W. J. MoberlyChan, R. M. Cannon, L. H. Chan, J. J. Cao, C. J. Gilbert, R. O. Ritchie, and L. C. De Jonghe, "Microstructural Development to Toughen SiC," Materials Research Society Proceedings, Boston, (1995).

73. W. J. MoberlyChan, J. J. Cao, and L. C. De Jonghe, "On the Role of Amorphous Grain Boundaries and the β - α Transformation to Toughen SiC," (in submission to *Acta Metall. Mater.*).

74. W. J. MoberlyChan, A. F. Schwartzman, J. J. Cao, and L. C. De Jonghe, "Phase Identification in SiC and Al_2O_3/SiC Composites Sintered with Al, B, and C," (to be submitted to *J. Matls. Sci.*).

75. C. J. Gilbert, J. J. Cao, W. J. MoberlyChan, L. C. De Jonghe, and R. O. Ritchie, "Cyclic Fatigue and Resistance-Curve Behavior of an *In Situ* Toughened Silicon Carbide with Al-B-C Additions, " (accepted by *Acta Metall. Mater.*).

76. H. J. Kleebe, "SiC and Si3N4 Materials with Improved Fracture Resistance," J. *European Ceramic Soc.*, **10**, 151-159 (1992).

77. M. K. Cinibulk, G. Thomas, and S. M. Johnson, "Grain-Boundary-Phase Crystallization and Strength of Silicon Nitride with a YSiAlON Glass," *J. Amer. Ceramic Soc.*, **73** [6] 1606-1612 (1990).

78. H. J. Kleebe, M. K. Cinibulk, R. M. Cannon, and M. Rühle, "Statistical Analysis of the Intergranular Film Thickness in Silicon Nitride Ceramics," *J. Amer. Ceramic Soc.*, **76** [8] 1969-1977 (1993).

79. J. McNaney and R. O. Ritchie, work in progress.

80. M. Mitomo, Y. Inomata, and M. Kumanomido, "The Effect of Doped Al on Thermal Stability of 4H- and 6H-SiC," *Yogyo-Kyokai-Shi*, **78**, [7] 224-228 (1970).

81. Y. Inomata, Z. Inoue, M. Mitomo, and H. Tanaka, "Polytypes of SiC Crystals Grown from Molten Silicon," *Yogyo-Kyokai-Shi*, **77**, [3] 83-88 (1969).

82. Y. Inomata, M. Mitomo, Z. Inoue, and H. Tanaka, "Thermal Stability of the Basic Structures of SiC," *Yogyo-Kyokai-Shi*, **77**, [4] 130-135 (1969).

83. Y. Inomata and Z. Inoue, "Wurtzite Type SiC Whiskers Obtained by Sublimation Method and the Thermal Stability of the Basic Polytypes of SiC," *Yogyo-Kyokai-Shi*, **78**, [4] 133-138 (1970).

84. C. Cheng, V. Heine, and R. J. Needs, "Atomic Relaxation in Silicon Carbide Polytypes," *J. Phys. Condensed Matter*, **2**, 5115-5134 (1990).

85. V. Heine, C. Cheng, and R. J. Needs, "The Preference of Silicon Carbide for Growth in the Metastable Cubic Form," *J. Amer. Ceramic Soc.*, **74** [10] 2630-2633 (1991).

86. Y. M. Tairov and V. F. Tsvetkov, "Progress in Controlling the Growth of Polytypic Crystals," in Prog. Crystal Growth and Characterization, ed. P. Krishna, Pergamon Press, **V7**, 111-161 (1983).

87. S. Martin, "Aspects of the Hot-Pressing of Silicon Carbide," Ph.D. Thesis, University of Cambridge (1980).

88. S. Yamada and M. Kumagawa, "Epitaxial Growth of SiC Using Al as an Accelerator," *J. Crystal Growth*, **9**, 309-313 (1971).

89. W. J. MoberlyChan, J. J. Cao, and L. C. De Jonghe, "Oversintering of SiC and SiC/Al_2O_3-Coated SiC-Platelet Composites", (to be submitted to *Comm. Amer. Ceramic Soc.*)

90. S. S. Shinozaki, J. E. Noakes, and H. Sato, "Recrystallization and Phase Transformation in Reaction-Sintered SiC," *J. Amer. Ceramic Soc.*, **61** [5] 237-242 (1978).

91. N. W. Jepps and T. F, Page, "The Etching Behaviour of Silicon Carbide Compacts," *J. Microscopy*, **124** [3] 227-237 (1981).

92. L. S. Sigl and H. J. Kleebe, "Core/Rim Structure of Liquid-Phase-Sintered Silicon Carbide," *J. Amer. Ceramic Soc.*, **76** [3] 773-776 (1993).

93. W. D. Kingery, H. K. Bowen, D. R. Uhlmann, Introduction to Ceramics, J. Wiley & Sons, 491-501 (1976).

94. B. W. Lin, M. Imai, T. Yano, and T. Iseki, "Hot-Pressing of β–SiC Powder with Al-B-C Additives," J. *Amer. Ceramic Soc.*, **69** [4] C67-C68 (1986).

95. J. Ruska, L. J. Gauckler, J. Lorenz, and H. U. Rexer, "The Quantitative Calculation of SiC Polytypes from Measurements of X-Ray Diffraction Peak Intensities," *J. Matls Sci.*, **14**, 2013-2017 (1979).

96. M. E. Sixta, J. J. Cao, W. J. MoberlyChan, and L. C. De Jonghe, "Oxidation Behavior of In-situ-Toughened SiC with Al, B, and C Additions," oral presentation at Amer. Ceramic Soc., Indianapolis, April, (1996).

97. J. J. Cao, Y. He, W. J. MoberlyChan, and L. C. De Jonghe, "Matrix-Grain-Bridging Contributions to the Toughness of SiC Composites with Alumina-Coated SiC Platelets," in Advances in Ceramic-Matrix Composites, Ceramic Transactions, Indianapolis, April (1996).

98. D. R. Clarke and G. Thomas, "An Optical Diffraction Study of the Stacking Sequences in Silicon Carbide," Electron Microscopy - (EMSA-1976), edited by G. W. Bailey, San Francisco Press, Inc., 492-493 (1976).

99. D. J. Smith, N. W. Jepps, and T. F. Page, "Observations of Silicon Carbide by High Resolution Transmission Electron Microscopy," *J. Microscopy*, **114** [1] 1-18 (1978).

100. M. Dubey, G. Singh, G. Van Tendeloo, "X-Ray Diffraction and Transmission Electron Microscopy of Extremely Large-Period Polytypes in SiC," *Acta Crystal.*, **A33**, 276-279 (1977).

101. N. W. Jepps, D. J. Smith, and T. F. Page, "The Direct Identification of Stacking Sequences in Silicon Carbide Polytypes by High-Resolution Electron Microscopy," *Acta Crystal.*, **A35**, 916-923 (1979).

102. M. A. O'Keefe and V. Radmilovic, "Extension of the 'Thin-Crystal' Condition by Small Crystal Tilts: Why HREM Images of SiC Polytypes Always Look Tilted," Electron Microscopy - (EMSA-1976), edited by G. W. Bailey, San Francisco Press, Inc., 116-117 (1992).

103. K. R, Kinsman and S, Shinozaki, "An Uncommon Mode of Morphological Development Among Coherent Phases (SiC)," *Scripta Metall.*, **12**, 517-523 (1978).

104. L. K. Frevel, D. R. Petersen, and C. K. Saha, "Polytype Distribution in Silicon Carbide," *J. Matls. Sci.*, **27**, 1913-1925 (1992).

105. R. M. Cannon and W. J. MoberlyChan, "Crystalline and Amorphous Triple Points in SiC," work in progress.

106. A. F. Bower and W. J. MoberlyChan, work in progress.

107. Y. Inomata, H. Tanaka, Z. Inoue, and H. Kawabata, "Phase Relation in SiC - Al_4C_3 - B_4C System at 1800°C," *Yogyo-Kyokai-Shi*, **88** [6] 353-355 (1980).

108. P. Dörner, "Constitution Studies in the High-Temperature Systems B-Al-C-Si-N-O with Help of Thermodynamic Calculations," Ph.D. Thesis, Institut für Metallkunde der Universität Stuttgart, Germany, 128-193 (1982).

109. Y. He, W. J. MoberlyChan, J. J. Cao, and L. C. De Jonghe, "Mg-Al Alloy as a Sintering Additive in Hot Pressed Silicon Carbide (SiC)," oral presentation at Amer. Ceramic Soc., Indianapolis, April, (1996).

110. H. Jagodzinski and H. Arnold, "Anomalous Silicon Carbide Structures," in Silicon Carbide, ed. J. R. O'Connor and J. Smiltens, Pergamon Press, 136-146 (1960).

111. P. Krishna and R. C. Marshall, "Direct Transformation From the 2H to the 6H Structure in Single-Crystal Silicon Carbide," *J. Crystal Growth*, **11**, 147-150 (1971).

112. W. S. Seo, C. H. Pai, K. Koumoto, and H. Yanagida, "Roles of Stacking Faults in the Phase Transformation of SiC," *J. Ceramic Society of Japan*, **100** [3], 227-232 (1992).

113. V. V. Pujar and J. D. Cawley, "Effect of Stacking Faults on the X-ray Diffraction Profiles of β–SiC Powders," *J. Amer. Ceramic Soc.*, **78** [3] 774-782 (1995).

114. C. S. Chang, I. S. T. Tsong, Y. C. Wang, and R. F. Davis, "Scanning tunneling microscopy and spectroscopy of cubic β–SiC (111) surfaces," Surface Science, **256** 354-360 (1991).

115. S. Tanaka, R. S. Kern, R. F. Davis, J. F. Wendelken, and J. Xu, "Vicinal and on-axis surfaces of 6H-SiC (0001) thin films observed by scanning tunneling microscopy," Surface Science, **350** 247-253 (1996).

116. J. W. Cahn, W. B. Hillig, and G. W. Sears, "The Molecular Mechanism of Solidification," *Acta Metall.*, **12**, 1421-1439 (1964).

117. W. A. Tiller, The Science of Crystallization: Microscopic Interfacial Phenomena, Cambridge University Press, 69-119 (1991).

118. S. Amelinckx and G. Strumane, "Surface Features on Silicon Carbide Crystal Faces," in Silicon Carbide, ed. J. R. O'Connor and J. Smiltens, Pergamon Press, 162-201 (1960).

119. A. R. Verma, "Polytypism and Surface Structure of Silicon Carbide Crystals - Interferometric and X-ray Studies," in Silicon Carbide, ed. J. R. O'Connor and J. Smiltens, Pergamon Press, 202-216 (1960).

120. Y. Inomata, "Crystal Chemistry of Silicon Carbide," in Silicon Carbide Ceramics V1, ed. S. Somiya and Y. Inomata, Elsevier Applied Science, 6 (1991).

121. F. C. Frank, "The Growth of Carborundum; Dislocations and Polytypism," *Phil. Mag.*, **42**, 1014-1021 (1951).

122. F. R. Chien, S. R. Nutt, W. S. Yoo, T. Kimoto, and H. Matsunami, "Terrace Growth and Polytype Development in Epitaxial β–SiC Films on α–SiC (6H and 15R) Substrates," *J. Mater. Res.*, **9** [4] 940-954 (1994).

123. H. S. Kong, J. T. Glass, and R. F. Davis, "Chemical vapor deposition and characterization of 6H-SiC thin films on off-axis 6H-SiC substrates," *J. Appl. Phys.*, **64** [5] 2672-2679 (1988).

124. H. S. Kong, J. T. Glass, and R. F. Davis, "Growth rate, surface morphology, and defect microstructures of β-SiC films chemically vapor deposited on 6H-SiC substrates," *J. Mater. Res.*, **4** [1] 204-214 (1989).

125. Z. Liliental-Weber, C. Kisielowski, S. Ruvimov, Y. Chen, J. Washburn, I. Grzegory, M. Bockowski, J. Jun, and S. Porowski, "Structural Characterization of Bulk GaN Crystals Grown Under High Hydrostatic Pressure," submitted to *J. Electronic Matls.*

126. A. F. Bower and M. Ortiz, "A Three-Dimensional Analysis of Crack Trapping and Bridging by Tough Particles," *J. Mech. Phys. Solids*, **39** [6] 815-818 (1991).

127. A. F. Bower, private communication.

128. W. D. Nix, private communication.

129. Y. Inomata, Z. Inoue, M. Mitomo, and H. Suzuki, "Relation Between Growth Temperature and the Structure of SiC Crystals Grown by Sublimation Method," *Yogyo-Kyokai-Shi*, **76**, [9] 313-319 (1968).

130. C. S. Smith, "Constitution and Microstructure of Copper-Rich Silicon-Copper Alloys," *Trans. AIME*, 313-333 (1940).

131. C. R. Houska, B. L. Averback, and M. Cohen, "The Cobalt Transformation," *Acta Metall.*, **8**, 81-87 (1960).

132. D. A. Porter and K. E. Easterling, in Phase Transformations in Metals and Alloys, Van Nostrand Reinhold Press, 404 (1981).

133. R. Hamminger, G. Grathwohl, and F. Thümmler, "Microanalytical Investigation of Sintered SiC: Part 2: Study of the Grain Boundaries of Sintered SiC by High Resolution Auger Electron Spectroscopy," *J. Matls. Sci.*, **11**, 3154-3160 (1983).

134. J. A. Powell and H. A. Will, "Low-Temperature Solid-State Phase Transformations in 2H Silicon Carbide," *J. Appl. Phys.*, **43**, 1400-1407 (1972).

135. J. P. Hirth and J. Lothe, in Theory of Dislocations, J. Wiley & Sons, (1982).

136. H. Jagodzinski, "Polytypism in SiC Crystals," *Acta Crystal.*, **7**, 300-305 (1954).

137. E. D. Whitney, "Polymorphism in Silicon Carbide," *Nature*, **199**, 278-280 (1963).

138. N. W. Jepps, Polytypism and Polytype Transformations in Silicon Carbide, Ph. D. Thesis, University of Cambridge (1979).

139. Y. C. Wang and R. F. Davis, "Growth Rate and Surface Microstructure in α-(6H)-SiC Thin Films Grown by Chemical Vapor Deposition," *J. Elect. Matls.*, **20** [10] 869-874 (1991).

140. D. R. Clarke, "On the Equilibrium Thickness of Intergranular Glass Phases in Ceramic Materials," *J. Amer. Ceramic Soc.*, **70** [1] 15-22 (1987).

141. I. Tanaka, H. J. Kleebe, M. K. Cinibulk, J. Bruley, D. R. Clarke, and M. Rühle, "Calcium Concentration Dependence of the Intergranular Film Thickness in Silicon Nitride," *J. Amer. Ceramic Soc.*, **77** [4] 911-914 (1994).

142. M. Akiyama and M. Yamamoto, "Silicon Carbide Whiskers (Tokawhiskers) and Their Application," in Silicon Carbide Ceramics V2, ed. S. Somiya and Y. Inomata, Elsevier Applied Science, 117-138 (1991).

143. J. Tafto and J. C. H. Spence, and P. Fejes, "Crystal Site Location of Dopants in Semiconductors Using a 100-KeV Electron Probe," *J. Appl. Phys.*, **54** [9] 5014-5015 (1983).

144. J. C. H. Spence and J. M. Zuo, in Electron Microdiffraction, Plenum Press, 131-134 (1992).

145. H. Yamauchi and H. Hasegawa, "Fabrication Method and Properties of β-SiC Ceramics" in Silicon Carbide Ceramics V2, ed. S. Somiya and Y. Inomata, Elsevier Applied Science, 183-196 (1991).

146. H. Kodama and T. Miyoshi, "Study of Fracture Behavior of Very Fine-Grained Silicon Carbide Ceramics," *J. Amer. Ceramic Soc.*, **73** [10] 3081-3086 (1990).

147. R. F. Davis, private communication.

148. A. Zangvil and R. Ruh, "Phase Relationships in the Silicon Carbide - Aluminum Nitride System," *J. Amer. Ceramic Soc.*, **71** [10] 884-890 (1988).

FIGURES

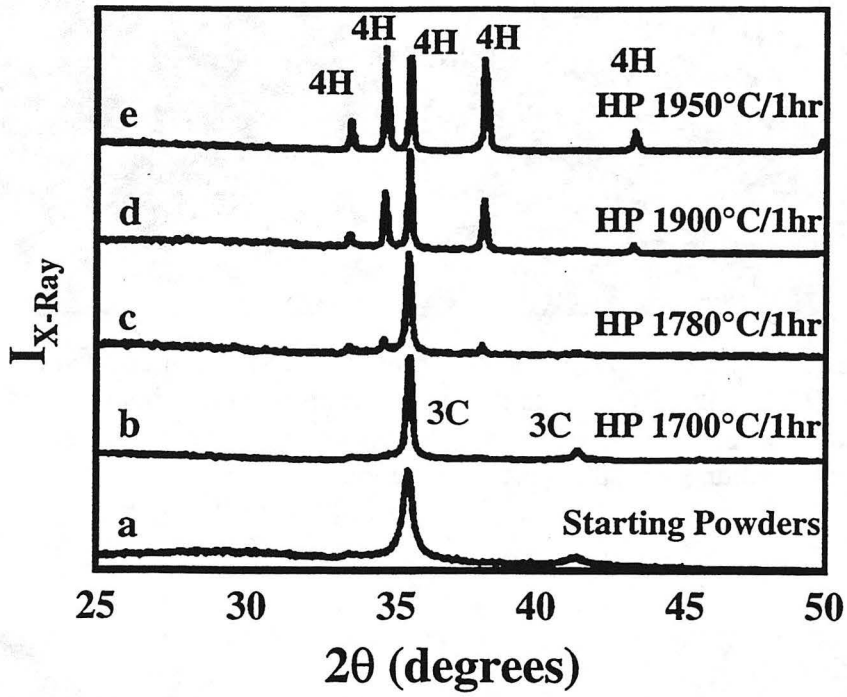

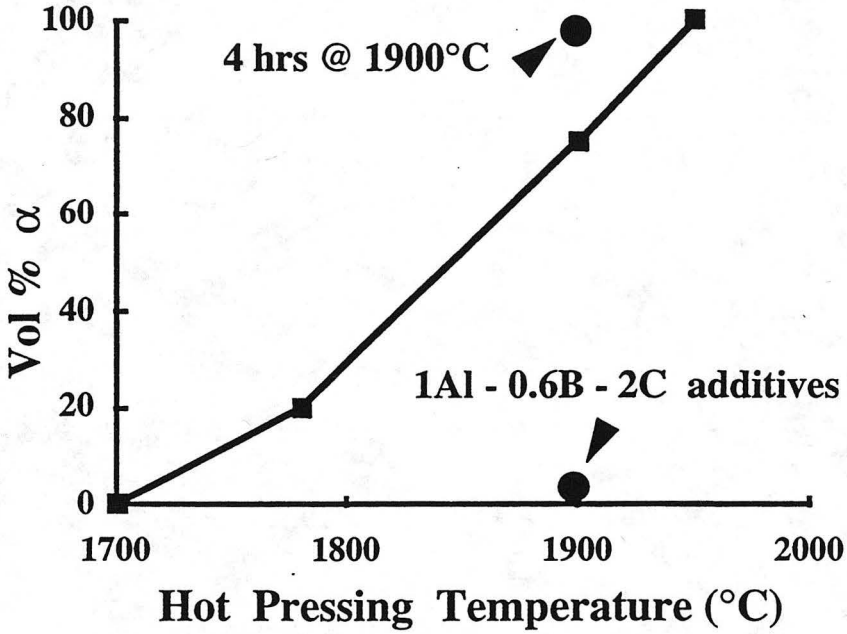

Fig. 1. X-Ray Diffraction scans of (a) the starting beta SiC powders and compacts hot pressed 1 hr at (b) 1700°C, (c) 1780°C, (d) 1900°C, and (e) 1950°C. Fig. 1f plots the volume fraction transformed to α as a function of temperature, for SiC processed 1 hr with 3% Al, 0.6% B and 2% C. Transformation is also dependent on time and additive concentrations; 4 hr at 1900°C with 3% Al produces full transformation, and 1 hr at 1900°C with 1% Al produces negligible α.

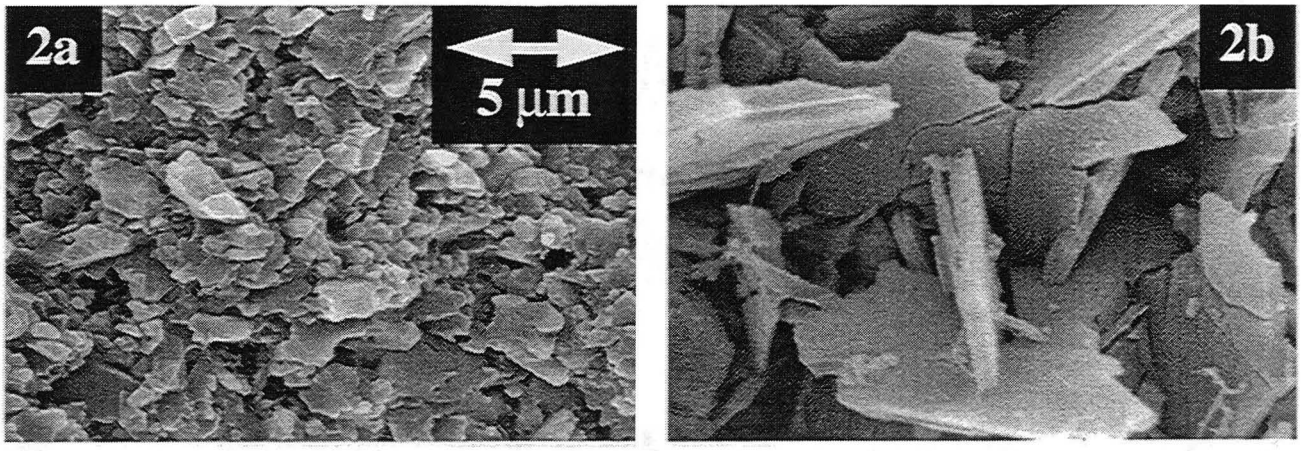

Fig. 2. SEM images of surfaces (etched in molten salt) of hot pressed SiC. After 1 hr at 1700°C (a) the SiC retains the cubic structure, yet grains begin to develop plate-like surfaces. Processing at 1900°C (b) produces an interlocking plate-like microstructure with the hexagonal structure.

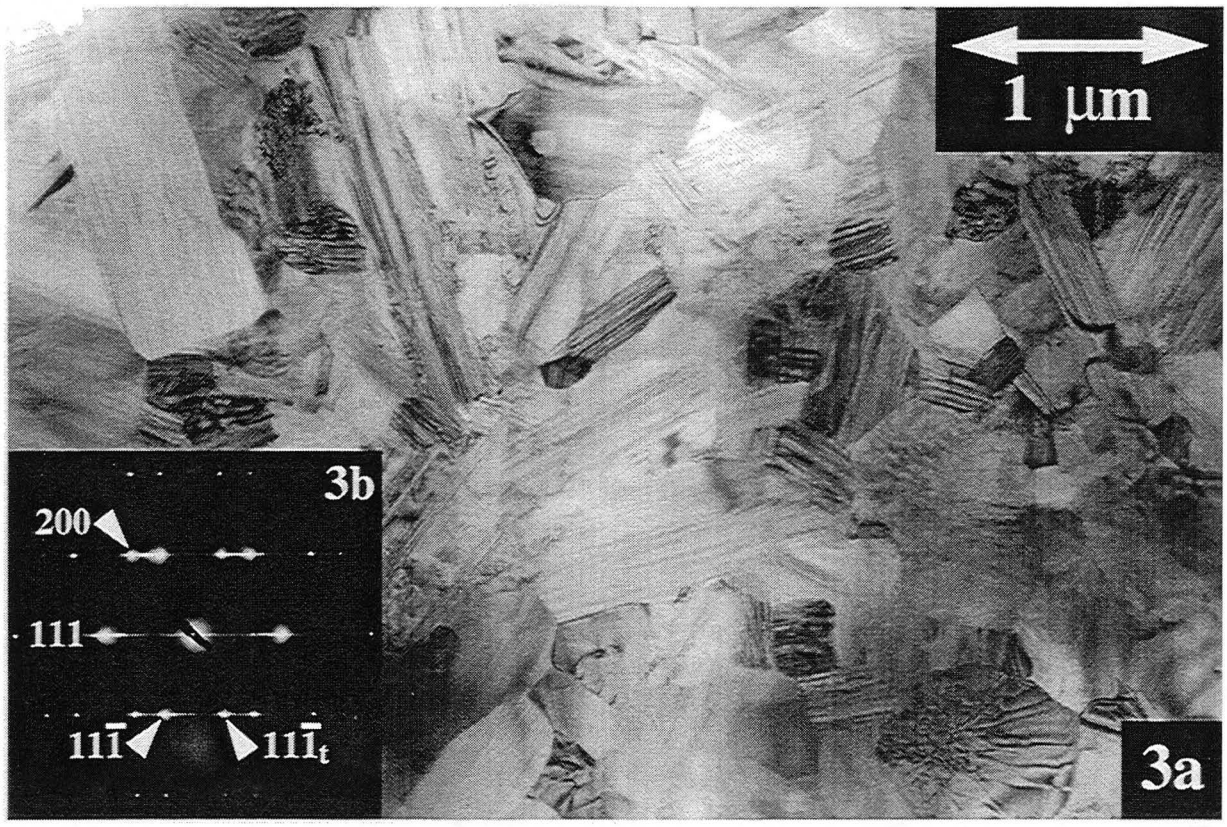

Fig. 3. (a) BF-TEM image of ABC-SiC (defined for the Al, B, and C additives) hot pressed 1 hr at 1700°C. Microtwins and stacking faults are parallel within each cubic grain, as indicated by twin reflections and streaking in the $[\bar{1}10]$ zone axis pattern (b).

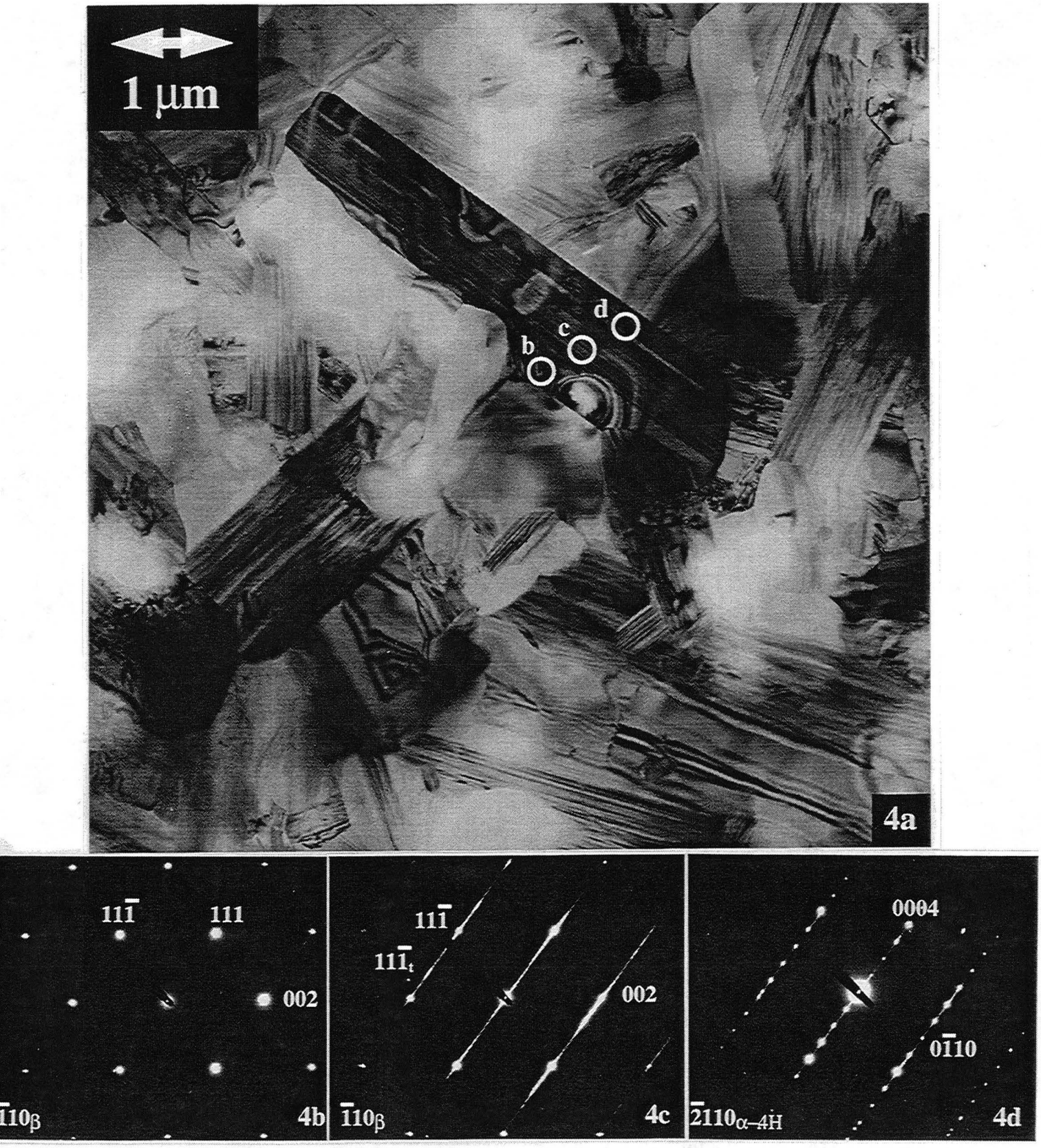

Fig. 4. (a) BF-TEM image of cross-sectioned, plate-like, dual-phase grain in ABC-SiC hot pressed 1 hr at 1780°C. SAD patterns determine the bottom (b) of the grain has the β-3C stacking, the top (d) has the α-4H structure, and the middle (c) has mixed structures, faults and microtwins. (ABC-SiC grains appear to grow in one direction, with the orientation of plate-like grains defined as follows: the "top" is flat, the "bottom" is rough, and the plate is horizontally elongated.)

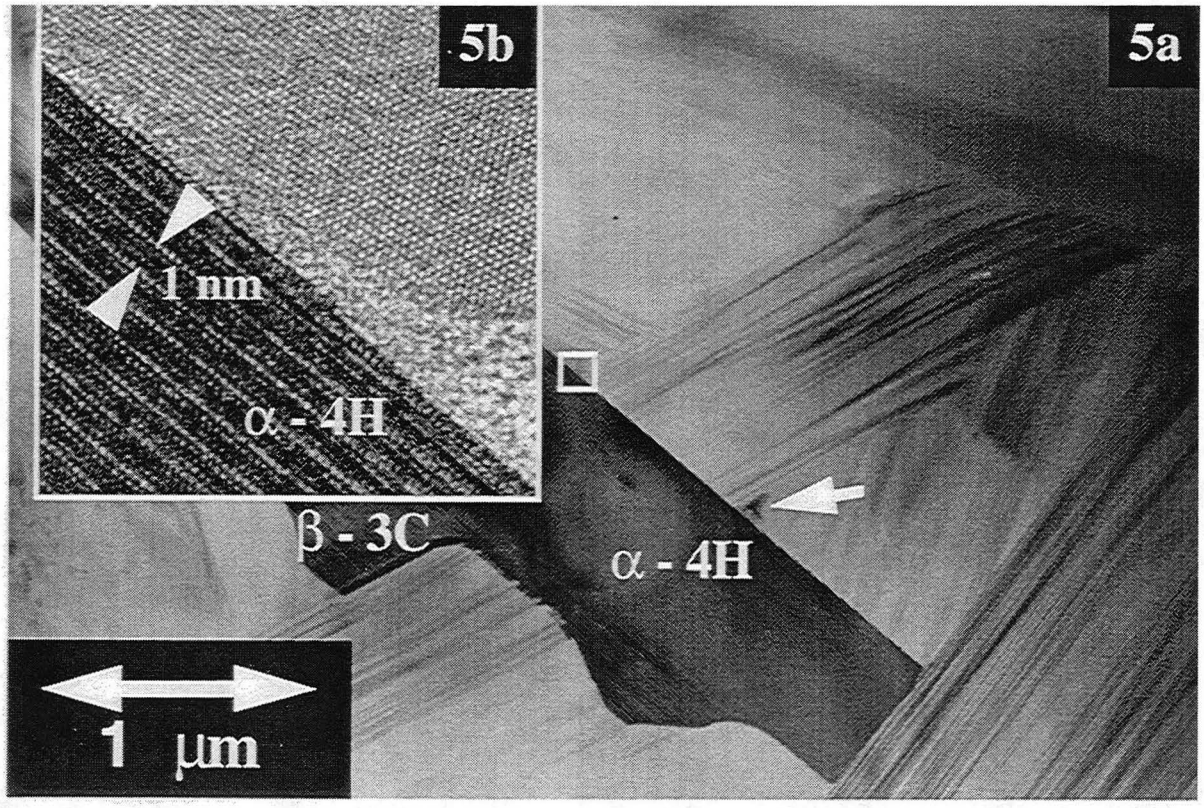

Fig. 5. (a) BF-TEM image of ABC-SiC hot pressed 1 hr at 1900°C, with diffracting grain oriented to the [$\bar{2}$110] zone axis. The top α-4H surface is atomically flat with HR-TEM (b) depicting a ~1 nm thick amorphous phase at grain boundaries; yet the bottom β-3C surface is irregular and faceted.

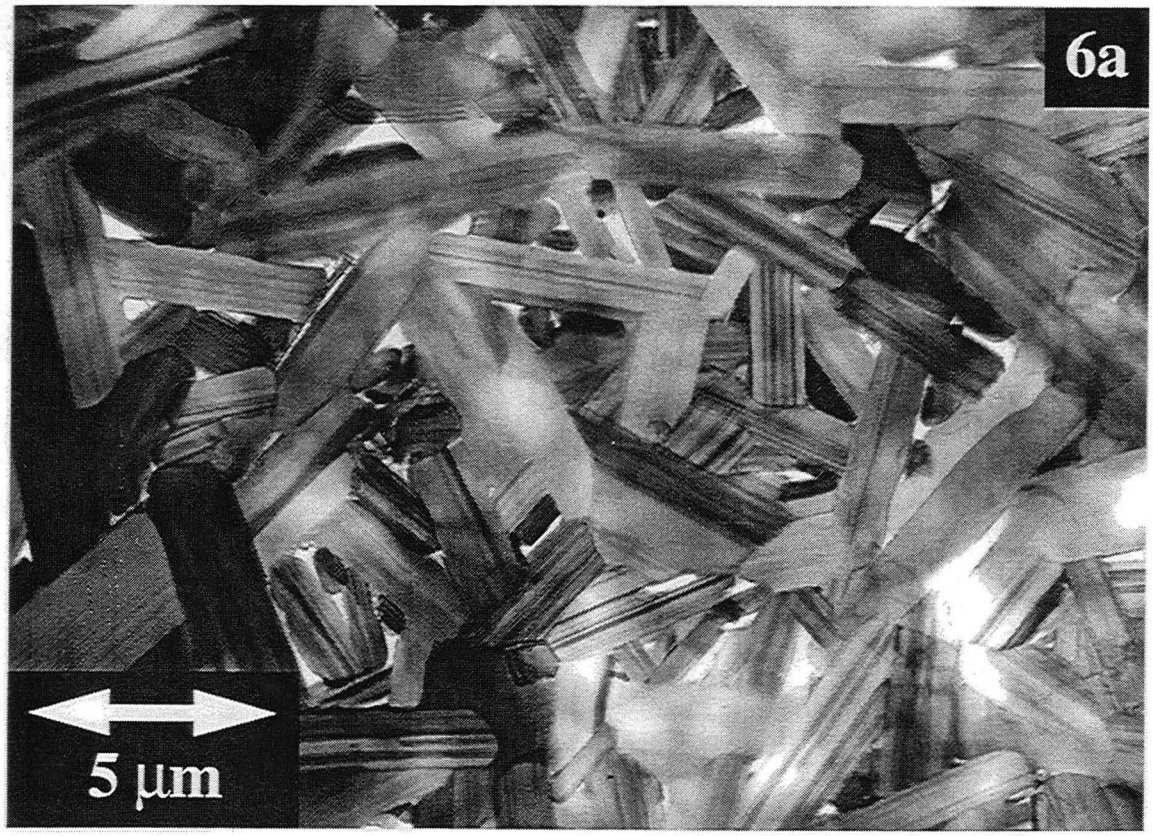

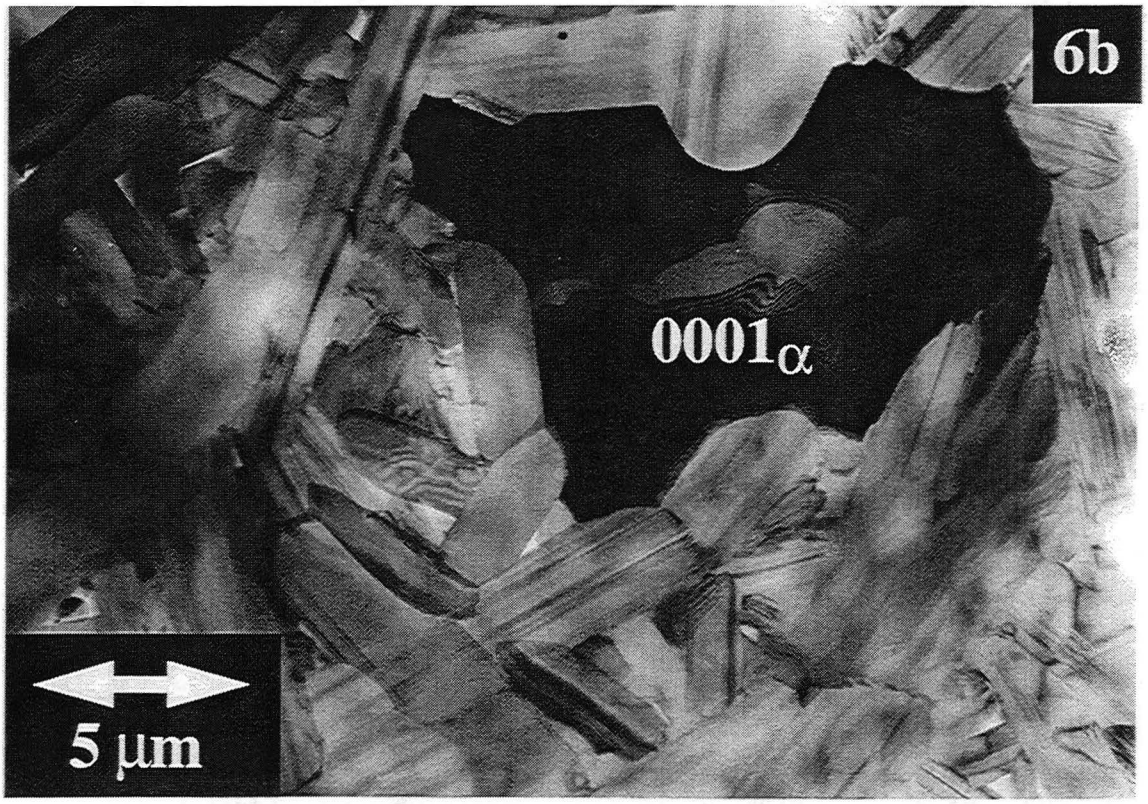

Fig. 6. (a) BF-TEM image of ABC-SiC hot pressed 1 hr at 1950°C. The aspect ratio of α-4H grains decreases when they grow at higher temperatures. Bright field image (b) acquired on [0001] zone axis depicts the irregular shape of the plate-like grain.

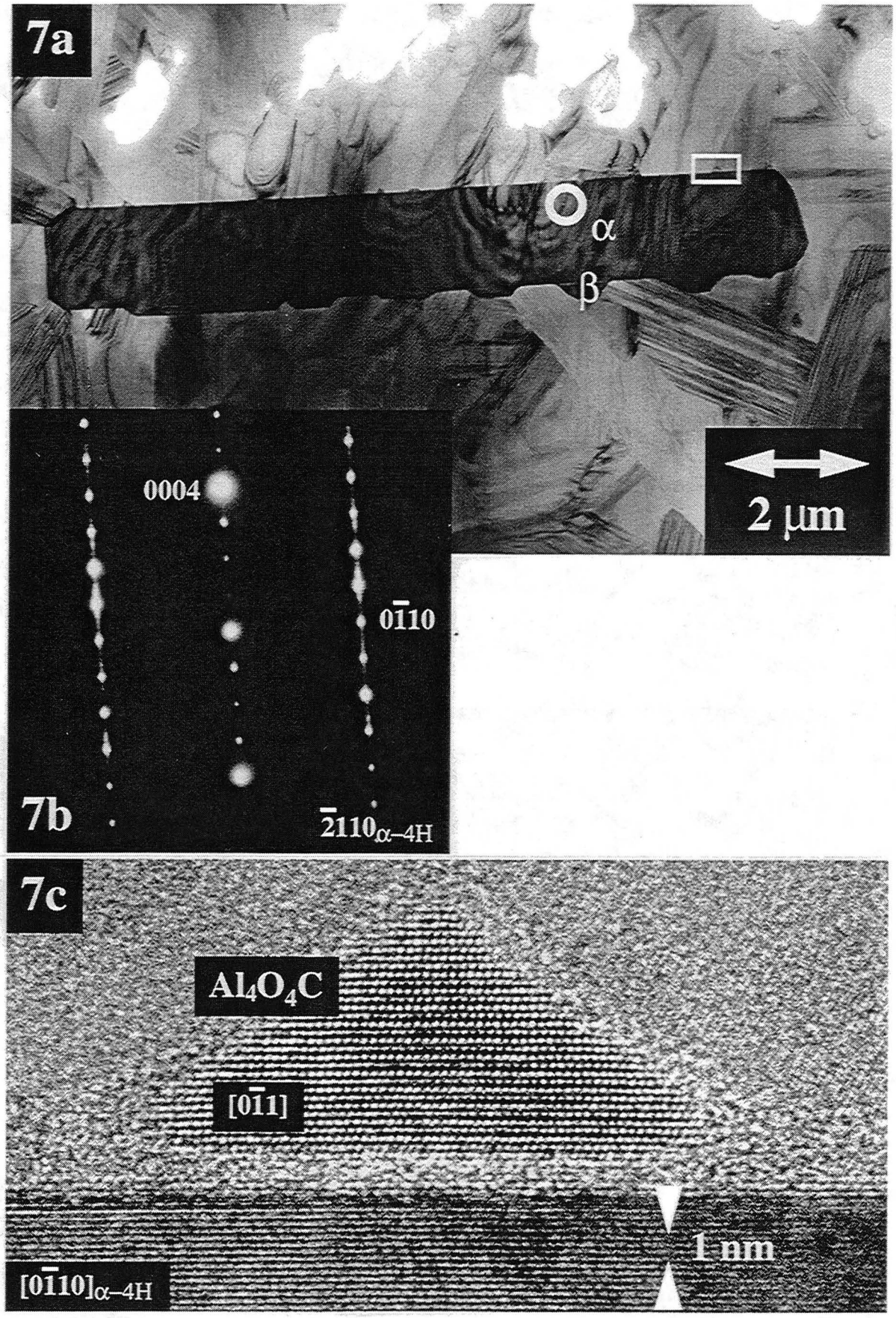

Fig. 7. (a) BF-TEM image of ABC-SiC hot pressed 4 hr at 1900°C. Faceted beta regions persist at the bottom of the plate-like grains. (In a general section of a plate-like grain, the beta-seed region is not imaged.) Stacking faults, denoted by streaking in SAD patterns (b), are less prevalent in the α-4H phase than in the β-3C phase. (c) HR-TEM image of crystalline triple point phase, similar to that denoted by box in Fig. 7a.

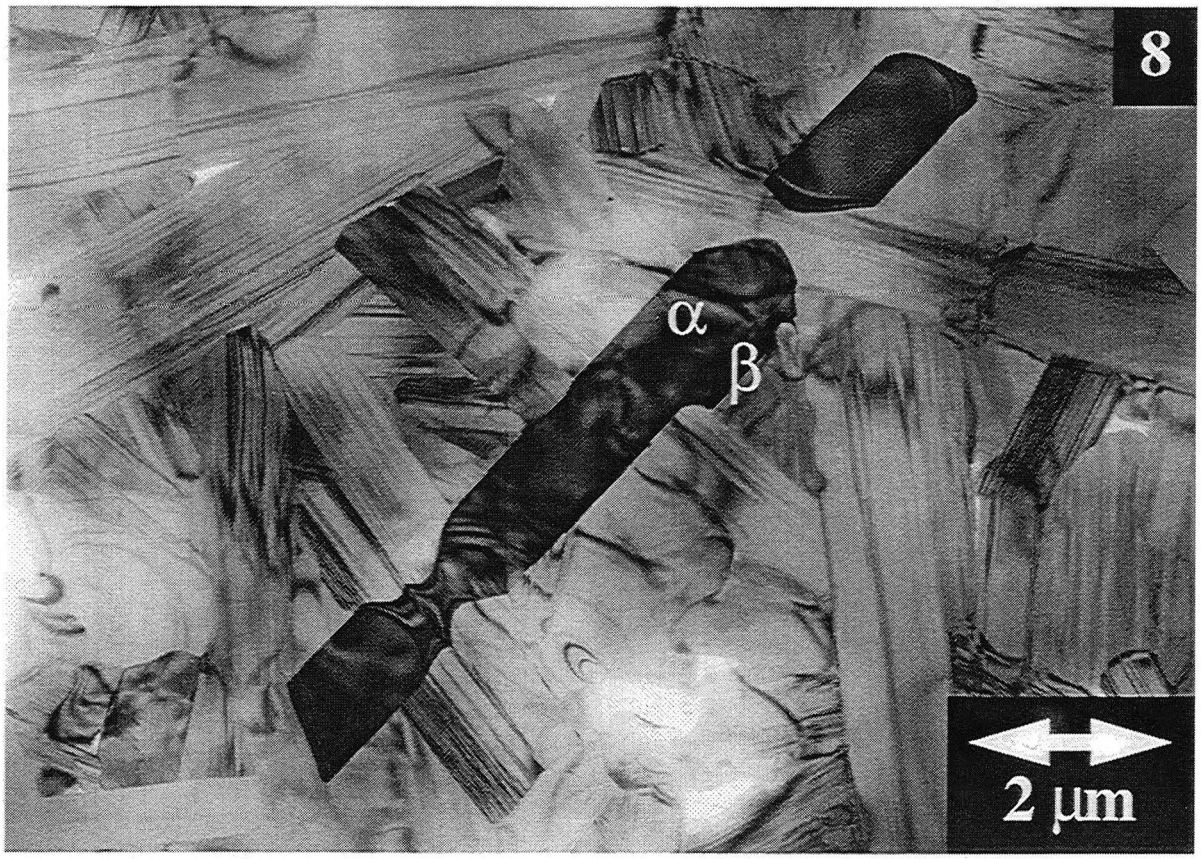

Fig. 8. BF-TEM image of dual-phase, plate-like microstructure of ABC-SiC (acquired on [$\bar{2}110$] zone axis). Strength increases [66, 68] as grains grow, due to enhanced interlocking as the aspect ratio increases.

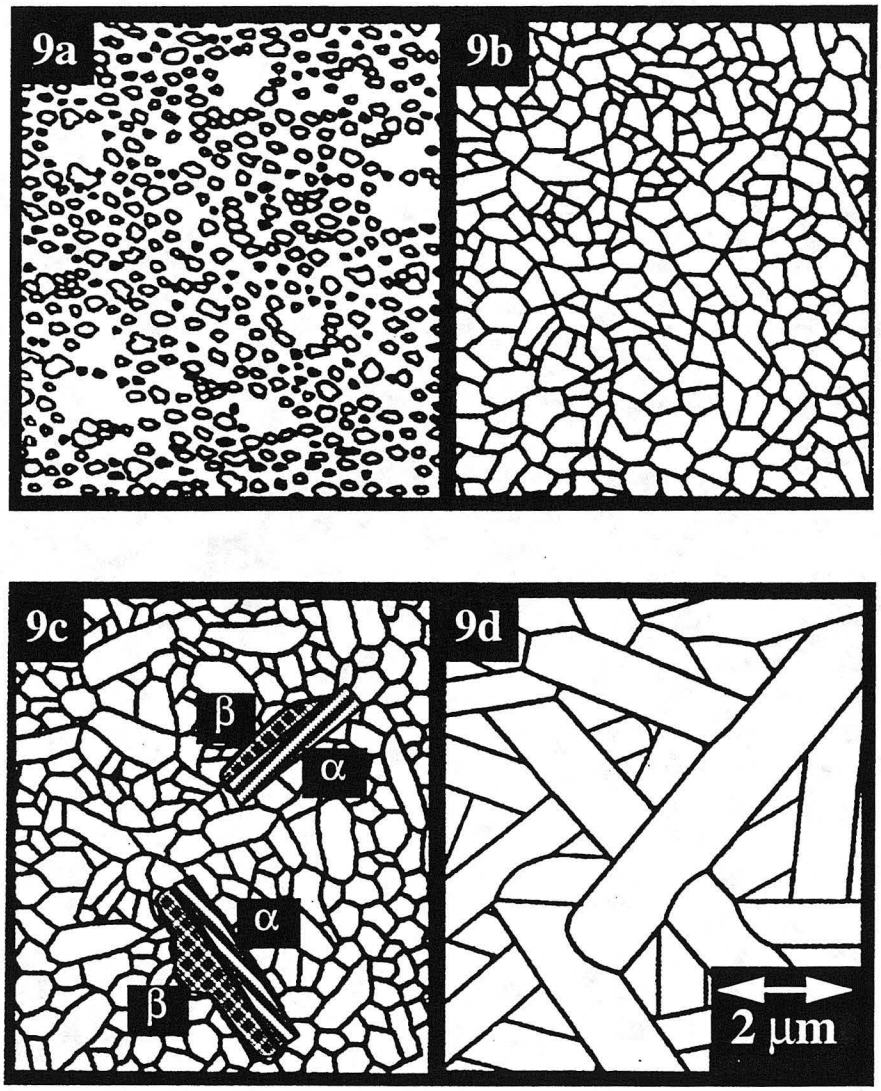

Fig. 9. Schematics of sintering / growth / transformation during SiC processing. (a) SiC powders densify (b) due to liquid-phase sintering. Growth of β-3C grains is asymmetric due to internal parallel faults, with growth perpendicular to the beta seed grain (c) switching to the thermodynamically preferred α-4H stacking. Dual-phase grains elongate (d) to produce an interlocked, plate-like microstructure.

Ernest Orlando Lawrence Berkeley National Laboratory
One Cyclotron Road ‡ Berkeley, California 94720

Prepared for the U.S. Department of Energy under Contract No. DE-AC03-76SF00098